INVESTIGATION OF REDOX-DEPENDENT BENTHIC NUTRIENT AND METAL FEEDBACKS UNDER ANOXIA USING EARLY DIAGENETIC MODELING

A THESIS SUBMITTED TO
THE GRADUATE SCHOOL OF NATURAL AND APPLIED SCIENCES
OF
MIDDLE EAST TECHNICAL UNIVERSITY

BY

KADİR BİÇE

IN PARTIAL FULFILLMENT OF THE REQUIREMENTS
FOR
THE DEGREE OF MASTER OF SCIENCE
IN
EARTH SYSTEM SCIENCE

JULY 2018

Approval of the thesis:

INVESTIGATION OF REDOX-DEPENDENT BENTHIC NUTRIENT AND METAL FEEDBACKS UNDER ANOXIA USING EARLY DIAGENETIC MODELING

submitted by **KADİR BİÇE** in partial fulfillment of the requirements for the degree of **Master of Science in Earth System Science Department, Middle East Technical University** by,

Prof. Dr. Halil Kalıpçılar _____
Dean, Graduate School of **Natural and Applied Sciences**

Prof. Dr. Can Bilgin _____
Head of Department, **Earth System Science**

Assoc. Prof. Dr. Mustafa Yücel _____
Supervisor, **Institute of Marine Sciences, METU**

Prof. Dr. Ayşen Yılmaz _____
Co-supervisor, **Institute of Marine Sciences, METU**

Examining Committee Members:

Prof. Dr. İsmail Ömer Yılmaz
Dept. of Geological Engineering/Earth System Science, METU _____

Assoc. Prof. Dr. Mustafa Yücel
Institute of Marine Sciences/Earth System Science, METU _____

Prof. Dr. Cemal Saydam
Department of Environmental Engineering, Hacettepe University _____

Date: _____

I hereby declare that all information in this document has been obtained and presented in accordance with academic rules and ethical conduct. I also declare that, as required by these rules and conduct, I have fully cited and referenced all material and results that are not original to this work.

Name, Last Name: KADİR BİÇE

Signature :

ABSTRACT

INVESTIGATION OF REDOX-DEPENDENT BENTHIC NUTRIENT AND METAL FEEDBACKS UNDER ANOXIA USING EARLY DIAGENETIC MODELING

BİÇE, KADİR
M.S., Department of Earth System Science
Supervisor : Assoc. Prof. Dr. Mustafa Yücel
Co-Supervisor : Prof. Dr. Ayşen Yılmaz

July 2018, 80 pages

Loss of oxygen in marine systems is a major management challenge that requires an integrated combination of watershed, water column and seafloor benthic (sediment) biogeochemical models. This challenge has not been successfully confronted yet. One of the primary reasons is the lack of understanding on the complex biogeochemical consequences of redox processes ocurring under anoxia. This thesis focuses on uncovering the complex effects of hypoxia/anoxia on sediment biogeochemistry and its feedbacks to the water column low-oxygen marine environments, taking the Black Sea as a model system. To do this, we have used a synthesis of early diagenetic modeling approaches from literature which are constructed upon reaction-transport modeling framework. Results about our simulations show that, with decreasing oxygen in bottom water, sediment becomes dominated with sulfate reduction and methanogenesis. Therefore, production of hydrogen sulfide and methane critically increases which represents the sulfidic conditions of the Black Sea. Results of metal ions show that, considerable amounts of Fe(II) and Mn(II) are also produced due to high organic

matter rain and less available oxygen. Flux estimates show that, deficiency of oxygen leads to lower phosphate and higher ammonia fluxes to the water column, thereby modifying the N/P ratio of the benthic-released nutrients. Under these conditions, if we assume that the mixing does not slow down as a result of warming, this feedback mechanism cause production of organic matter to increase further which leads to a more critical future deoxygenation.

Keywords: Marine sediment biogeochemistry, early diagenesis, reaction-transport modeling, hypoxia, anoxia, the Black Sea

ÖZ

ANOKSİK KOŞULLARDA REDOKSA BAĞLI BENTİK BESİN VE METAL DÖNGÜLERİNİN ERKEN DİYAJENEZ MODELLEMESİ İLE İNCELENMESİ

BİÇE, KADİR
Yüksek Lisans, Yer Sistem Bilimleri Bölümü
Tez Yöneticisi : Doç. Dr. Mustafa Yücel
Ortak Tez Yöneticisi : Prof. Dr. Ayşen Yılmaz

Temmuz 2018 , 80 sayfa

Deniz sistemlerindeki oksijen kaybı havza, su kolonu ve deniz tabanı (sediman) modellerinin birleşimiyle çalışılması gereken önemli bir yönetim problemidir. Bu problem üzerine şu ana kadar yeterli miktarda çalışılmamıştır. Bunun altında yatan başlıca etkenlerden biri de redoks süreçlerinin sonucu olarak oluşan karmaşık biojeokimyasal döngülerin yeterli miktarda anlaşılmamış olmasıdır. Bu tez, düşük oksijenli Karadeniz'i örnek bir sistem alarak hipoksi/anoksinin sediman biojeokimyası ve bunun su kolonuna olan geri dönüşleri üzerinde etkilerini araştırmaya odaklanmaktadır. Bunu yapabilmek için, literatürde bulunan reaksiyon-taşınım modelleri üzerine kurulu erken diyajenez modellenmesi çalışmalarının birleşimi olan bir yaklaşım kullanılmıştır. Simulasyon sonuçlarımız oksijen azlığında sediman biojeokimyasında sülfat indirgenmesi ve metan oluşumunun baskın hale geldiğini göstermektedir. Bundan dolayı, hidrojen sülfür ve metan üretimi artarak Karadeniz'in sülfidik ortamını temsil etmektedir. Metal iyonları ile ilgili sonuçlar, organik karbon yağışı ve oksijen azlığı sebebi

ile ciddi miktarda Fe(II) ve Mn(II) üretimi olduğunu göstermektedir. Akış tahminleri, oksijen azlığında su kolonuna çıkan besin kaynaklarının arttığını göstermektedir. Bu koşullar altında, su kolonunda ısınmadan etkilenmeden düzgün işleyen bir karışım olduğunu varsayarsak, bu geri bildirim mekanizması organik karbon üretimini daha da arttırarak ileriki zamanlarda daha kritik bir oksijensizleşmeyi tetikleyebilir.

Anahtar Kelimeler: Deniz sedimanı biojeokimyası, erken diyajenez, reaksiyon-taşınım modellemesi, hipoksi, anoksi, Karadeniz

To my family

ACKNOWLEDGMENTS

First, I would like to thank my supervisor Assoc. Prof. Dr. Mustafa Yücel for his continuous support throughout my thesis study. His friendly and caring behaviour motivated me to enter the World of Marine Sciences and pursue a PhD in this field. Also, his hospitality in the IMS METU made me a part of this beautiful community. It was a pleasure to work with him and I hope to continue with collaborations in the future.

Besides, I would like to thank my co-advisor Prof. Dr. Ayşen Yılmaz for her effort to draw my interest on the Earth System Science and then Marine Sciences at the very beginning. She was the one who directed me to interdisciplinary studies therefore her impact on this study is very important.

Additionally, I would like to thank Prof. Dr. İsmail Ömer Yılmaz and Prof. Dr. Cemal Saydam for their valuable evaluations and contributions in my thesis defense. I would also like to thank Dr. Karline Soetaert for providing an open access implementation of the OMEXDIA model.

Furthermore, I am also grateful to all of my friends for their endless support and motivation in every step of this process. Specially, I would like to thank Nilgün Efe for her unique support and continuous encouragement. I would also thank my lab friends Duygu Pamukçu and Nur Banu Demir.

Finally, I must express my very profound gratitude to my parents and my brother for their constant love and support throughout this process. It would be impossible for me to do this study without them.

TABLE OF CONTENTS

LIST OF TABLES

TABLES

LIST OF FIGURES

FIGURES

LIST OF ABBREVIATIONS

AOM	Anaerobic Oxidation of Methane
BW	Bottom-Water
CBD	Convention on Biodiversity
CIL	Cold Intermediate Layer
FPL	Fine Particle Layer
ISA	International Seabed Authority
OAE	Ocean Anoxic Events
ODE	Ordinary Differential Equations
ODU	Oxygen Demanding Units
OM	Organic Matter
SWI	Sediment-Water Interface

CHAPTER 1

INTRODUCTION

Biogeochemical cycles of the Earth System operate in a multitude 'spheres' that work in a harmony to provide and sustain the habitability. In general sense, they can be listed as: atmosphere, hydrosphere, lithosphere and biosphere. For hundreds of million years, these factors interacted with each other to reach a chemically stable environment for the life [1]. Today, the Earth as a whole still continues to regulate conditions for the survival of the living organisms as proposed by James Lovelock in his well-known work 'GAIA'.

In recent decades, with increased anthropogenic forcing, the Earth has started to enter into series of critical changes. These changes are mainly due to the alterations in the composition of the atmosphere which resulted into the global warming. In contrast to the naturally occurring events in the past (i.e. volcanic activities, ice ages), main reason behind the current global warming is the human caused emissions which interferes with the ability of atmosphere to keep the Earth cooler [2]. In the first half of the 20th century, it is estimated that the mean global temperatures increased by 0.2°C [3] and in last 30 years, it is increased by 0.2°C per decade [4]. Other than emitting excess amount of gas to the atmosphere, human activities such as deforestation and desertification are also effective on this process of heating [5]. Figure 1.1 shows a World map and a graph showing surface temperature anomalies between 1951-1980 period and current conditions. In this figure, it is clearly seen that especially high latitudes experience abnormal amounts of heating.

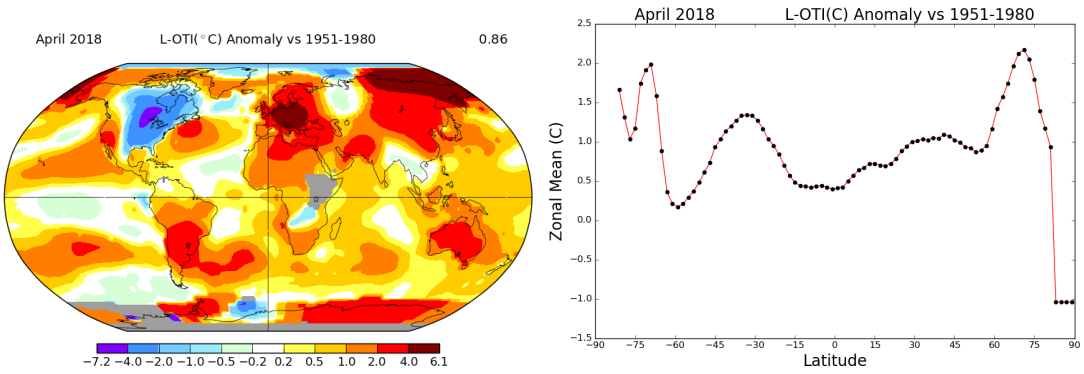

Figure 1.1: Global Temperature Anomalies Map and Graph [Credit: NASA Goddard Institute for Space Studies]

Together with the heating of the Earth, global biogeochemistry is also being affected by human induced changes. Since the global biogeochemistry is strongly connected to all spheres of the Earth, any negative change triggers unpredictable feedbacks in the long run [6]. Under these conditions, some of these spheres has already started to give signals for possible drastic future effects.

In recent years, studies showed that oceans are one of the most crucial places where negative changes occur [7]. Oceans are critical to global biogeochemistry due to their role in the biogeochemical cycles of main species such as C, N, O and S. In terms of carbon cycle, they are unique sinks for the CO_2 with a 48% of the total CO_2 originating from fossil fuel emissions [8] and even more potential sink in polar oceans due to high production and low temperature [9]. Since the land on the surface of the Earth is surrounded by bodies water, marine environment became one of the most vulnerable among these environments because of its inevitable fate of becoming a global deposit site for the solid and liquid outputs produced by humankind. According to [6], there are three major threat to the oceans: ocean warming, ocean acidification and ocean deoxygenation. In this study, we focus on ocean deoxygenation and oxygen related conditions in the marine environment: anoxia and hypoxia.

1.1 Anoxia and Hypoxia in Marine Environment

Oxygen (O_2) is an important chemical species for living organisms to sustain their living also in marine environment. It is the most powerful oxidant of the thermodynamic redox ladder in organic matter mineralization reactions and also the only oxidant for aerobic organisms [10]. Therefore, it has a crucial role in survival of the marine life as well as marine biogeochemistry. O_2 is a critical factor in biogeochemical cycling in the marine environment as oxic processes are strongly coupled to C, N, P, Fe and other redox-sensitive elemental cycles [6]. One example can be denitrification which takes place in the absence of O_2 and is crucial for removal of a primary production limiting nutrient N [11]. Additionally, oxygen related conditions in the past such as ocean anoxic events (OAE) are important for the assessment of paleoproductivity and biogeochemical cycles in the past [12].

In highly populated areas, organic matter input to the coastal seas are high which increase biogeochemical demand for O_2. As a result, oceans and coastal marine environments are prone to the risk of 'anoxia'. This phenomenon can be defined as the lack of dissolved O_2 in the water. Aside from the relatively minor temperature effect on oxygen solubility, the main factor leading to anoxia is the depletion of O_2 by microbial activity. This process of O_2 depletion is mainly caused by the decrease of O_2 supply to the water column due to lower mixing and advection. Warming of oceans because of the atmospheric heat is the key element of this mechanism. Alongside with atmospheric heating, heating of oceans decreases solubility of O_2 and also increases stratification which weakens mixing of O_2 to deeper waters [6]. Additionally, increased temperature enhances metabolic activities and respiration leading to higher consumption of oxygen [13]. Estimations on effect of warming on O_2 levels suggest that global ocean would lose 6 nmol of O_2 for one joule of heat on average [14]. Another estimate in [15] shows that under constant biological uptake, a 1°C increase in ocean would make ocean to lose $9.4 * 10^{15}$ moles of O_2 and therefore increase atmospheric O_2 by 0.026%.

Besides ocean warming, nutrient input to the ocean is another important factor triggering anoxia in coastal waters. It can be done by land runoff or by atmospheric deposition which are controlled by factors such as precipitation, wind, storm and land-cover [16, 13]. After high nutrient supply, eutrophication occurs which can be defined as the boost of primary production due to high nutrient input [10]. Increasing primary production leads to increase in biological population and therefore particulate organic matter raining towards the seafloor. Since organic matter and O_2 are the primary resources of the aerobic respiration, this increase in organic matter leads to the excess usage of O_2. Therefore, O_2 and organic matter are used until depletion. In nutrient rich and stratified waters where human activity is high, organic carbon rain is strong enough to deplete O_2 therefore, deep waters and sediment becomes hypoxic or anoxic (Figure 1.2). According to [17], there are several degrees of eutrophication-based hypoxia depending on the duration: seasonal (50%), periodic (25%), episodic (17%) and persistent (8%). In todays Earth, seasons are stretching with the warming therefore, seasonal hypoxia which is a crucial part of the total can be more important with this trend [13]. In any of these types, there is a potential to cause even worse feedback mechanisms such as flux of hydrogen sulfide and methane from the sediment to the water column [18].

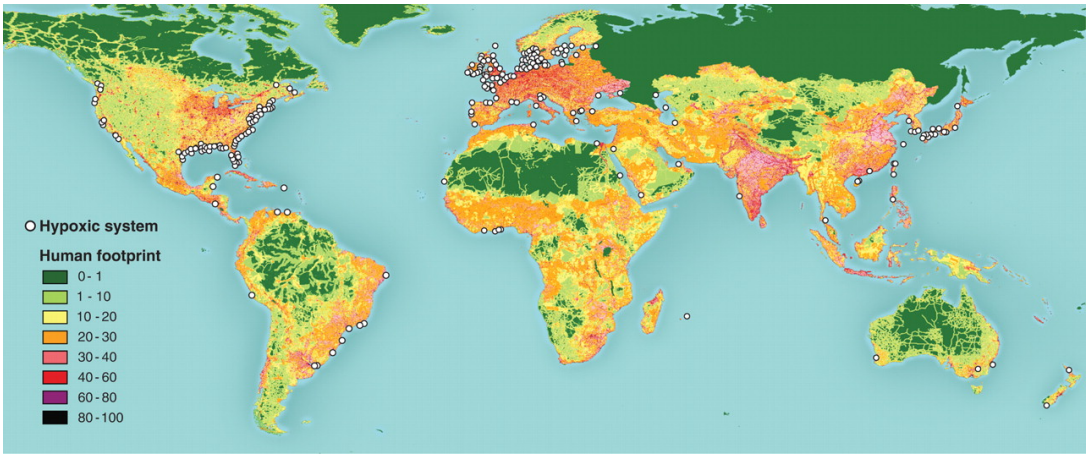

Figure 1.2: Hypoxia and Human Activities [17]

Potential impacts of ocean deoxygenation would be devastating for the marine life.

Studies show that, anoxic deep waters were critical in several mass extinction events in the past due to high hydrogen sulfide output to the atmosphere [19]. Effects of anoxia could be doubled by a combination with eutrophication and change in ocean currents which would increase degradation of benthic communities [20]. Additionally, a study on thresholds of hypoxia caused mortalities shows that dissolved oxygen becomes dangerous under 2 mg/liter and critical under 0.5 mg/liter [21]. Other than direct mortality problems, hypoxia/anoxia has a potential to expedite another global issue which is the ocean acidification [22].

Marine sediments are critical to the ocean anoxia/hypoxia since they gather the organic carbon rain and have benthic communities for the biogeochemical cycles of nutrients. Near-surface parts of the sediments can have more biogeochemical interactions compared to the whole water column [23]. In this study, our focus is on anoxia/hypoxia in marine sediments and we consider early diagenesis to study dynamics of species under anoxia and possible effects on the water column.

In this study, we focus on the Black Sea because of its unique structure allowing us to simulate anoxic and suboxic conditions. The Black Sea has a estuarine-like circulation and supply of O_2 is dependent on the ventilation of the cold intermediate layer (CIL) therefore, CIL is an important parameter affecting bottom-water O_2 concentrations [24]. Another important factor affecting bottom water concentrations is the fine particle layer (FPL) where, co-existance of phosphate minimum along with the depletion of ammonia, Mn(II) and methane occurs [25].

Additionally, the Marmara Sea is also another unique system that is considered in this study which has developing hypoxic conditions due to high anthropogenic input. The Marmara has two straits which supply more saline Mediterranean deep waters and less saline Black Sea surface waters which creates a pycnocline preventing mixing between layers. In addition, it has a jet-like flow entering from Bosphorus due to fresh water input from the Black Sea which creates an anticyclone [26].

1.2 Early Diagenesis in Marine Sediments

According to [27], early diagenesis refers to the sum of all physical, chemical and biological dynamics within a short period of time and shallower depths excluding long term burial activities. These changes are due to presence of pore-water which acts as an intermediate medium for transport and biogeochemical reactions. Since early diagenesis is limited in time and depth, it does not consider significant changes in temperature and pressure therefore deep burial and metamorphosis activities are out of scope of this framework. Study of early diagenesis is divided into 3 types: instrumentation, laboratory and theoretical/mathematical modeling [27]. Instrumentation includes studies where in-situ measurements are performed to obtain data regarding chemical concentrations and fluxes. Laboratory experiments are done to observe changes in controlled environment. Theoretical/mathematical modeling focuses on quantifying interplays between system components and estimations of the future behavior of the system. From experimental perspective, these tasks are difficult or impractical to perform since experimental approaches mostly focus on net measurements instead of future interactions. Additionally, diagenetic processes require very long times to be observed using experimentations [28]. To make correct estimations, theoretical modeling is dependent on data generated in-situ and in laboratory experiments therefore, combination of these approaches are needed to be able to study early diagenesis. In this framework, we focus on theoretical modeling part to estimate effects of anoxia/hypoxia on sediments and potential feedbacks to the water column.

1.2.1 Early Diagenetic Modeling

Theoretical modeling of early diagenesis which is called as 'early diagenetic modeling' is firstly introduced by [27] and improved by several classical studies such as [29, 30, 28, 31]. Early diagenetic modeling basically is a subset of reactive transport

modeling which focuses on transport and chemical reactions of certain species in different settings. These settings include environmental systems such as marine, estuarine and groundwater systems as well as engineering systems such as waste water treatment plants. Similar to the regular reactive transport models, a general diagenetic equation considers changes in the following parts as defined by [27]:

$$Concentration = Diffusion + Bioturbation - Advection + Reaction \quad (1.1)$$

This equation can be solved to steady-state where concentration change according to time is zero or to a transient state where time specific simulation is needed. Product of this modeling approaches generally include depth profiles of concentrations of certain species as in Figure 1.3.

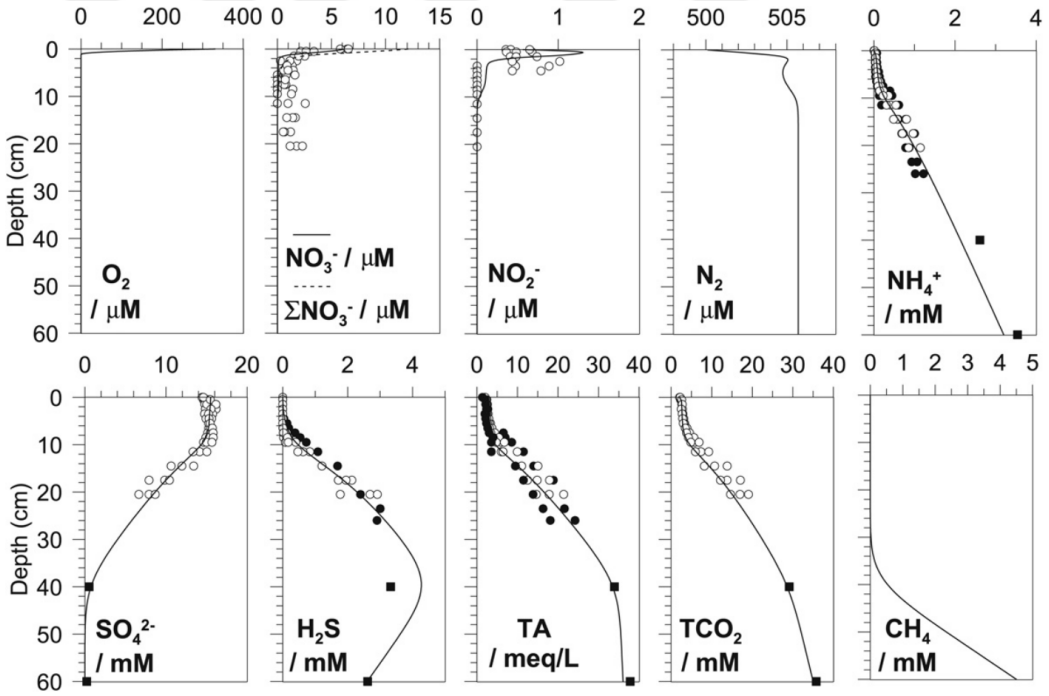

Figure 1.3: Sample Depth Profiles for Redox Species [32]

In literature, starting from 1996, there exists several diagenetic modeling studies which differ from each other in terms of these factors: extent of transport processes, organic matter pools with different reactivities, formulation of organic matter oxida-

tion pathways with rate laws and parameters, secondary redox reactions and mineral formation reactions [33].

Transport in early diagenetic modeling may include diffusion, bioturbation, bioirrigation and advection. Diffusion is a molecular property depending on concentration differences, porosity, and diffusion coefficients therefore, it has no velocity component. Diffusion coefficients for solutes in sediments are calculated depending on temperature, salinity and pressure. Additionally, since sediments are composed of mixture of liquid and solid phases, tortuosity is also a factor affecting diffusion coefficients [27].

Bioturbation is defined as the mixing of particles in sediment by local animals [34]. In sediments, it is frequently constructed as a depth-dependent parameter [35]. Although, bioturbation coefficient for solutes and solids are generally taken as the same, some researchers argue that bioturbation of a solute is 10 times larger than of solids [36]. Apart from phase difference, availability of oxygen is also taken as a controlling factor on bioturbation in a study [37]. Bioirrigation is also a mixing activity done by irrigating worms. In some studies it is directly omitted due to anoxic/hypoxic conditions causing degraded macrofauna [38] and in another study, magnitude of bioirrigation is inversely estimated using measured O_2 concentration [39].

Advection is a transport process due to the flow of the surrounding medium. In sediments, it is related to the pore-water velocity which may depend on burial, compaction or hydrological flow [28]. In most of the studies, burial is taken as the main advective transport and it can differ for solids and solutes.

In early diagenetic modeling, reactivity of the organic matter is also important alongside with the availability. In most of the models, there are multiple organic matter pools with different rates of decomposition into CO_2. This approach is proposed by [27] as 'multi-G' model and still in use by many modeling studies. In [40], they focus on the proportion of the reactive OM reaching to the seafloor instead of only focus-

ing on the reactivity constants. Another alternative exists as 'continuous-G' where properties of an organic matter changes by depth, representing the age of the organic carbon [41].

Other than reactivity of organic matter, redox pathways are also important in early diagenetic modeling. In most of the studies, redox pathways are modeled as introduced by [42] with all of the primary redox species: O_2, NO_3, MnO_2, $FeOH_3$, SO_4 and CH_4 but potentially with different organic matter stoichiometry. In some of the studies, anoxic mineralization processes are lumped into one reaction and resulting species are called as oxygen demanding units (ODU) [30]. In formulation of redox reactions, a common approach is to calculate rate expressions as multiplication of reaction rate of organic matter, limitation and inhibition terms. Additionally, some studies include temperature dependence, microbial biomass and thermodynamic factor [43]. In most studies, limitation and inhibition terms for oxidants are Monod expressions which include Monod half saturation and inhibition constants as proposed in [44]. Some studies, such as [45] use Monod expressions also for reaction rate of the organic matter.

In early diagenetic models, secondary redox and mineral reactions are important for cycling of nutrients and resupply of oxidants. Species range in these reactions may include: NH_4^+, $Mn^{4+,3+,2+}$ Fe^{2+}, H_2S, CH_4, FeS, FeS_2, ODU and S^0 [33]. In literature, secondary redox reactions are mostly formulated as second order. Different from them, in mineral formation and dissolution, second order kinetics or pH dependent approaches are used since minerals are sensitive to pH of the water. In most of the models, pH of the water is calculated using 'alkalinity conservation' approach as in [31]. Other than these reactions, adsorption of NH_4 and PO_4 are modeled with fixed ratios [30, 46] or as adsorption to iron [38, 47, 48].

In early diagenetic modeling literature, there exists many different models from all levels of complexities. Models presented in these studies are tailored to serve as a

research tool to investigate aimed research questions. In this study, we use a relatively simple 1D early diagenetic model with more focus on biogeochemistry side which is created upon existing models to study impact of anoxia/hypoxia on marine sediments. In literature, there are extensive ecosystem models considering anoxia/hypoxia and early diagenesis [49, 50] however, in our study we aim to understand changes in depth profiles and fluxes under variable levels of oxygen using a more 'biogeochemistry-oriented' early diagenetic model. More specifically; my thesis will pursue the following objectives:

1. Create depth profiles of primary and secondary redox species to observe impacts of anoxia on sediment biogeochemistry
2. Estimation of feedbacks to the water column under anoxia such as nutrient and metal fluxes
3. Synthesize a basic model to be used as a tool to understand sediment biogeochemistry in future studies of the Black Sea and the recently deoxygenating Marmara Sea

The remainder of this study is structured as follows. In Chapter 2, material and methods used to test the research questions are listed. In Chapter 3, the simulation results are presented, the outcomes of diagenetic model predictions including fluxes, mineralization rates are discussed, and more general implications are made. In Chapter 4, we conclude with key findings and present future directions of this study.

CHAPTER 2

MATERIAL AND METHODS

2.1 Early Diagenetic Model

In testing our research questions, we used an hybrid approach which combines modeling framework used in [46] which is a more complex version of earlier studies [35, 28] and the open source early diagenetic model OMEXDIA [30]. We used the general structure of OMEXDIA which is based on the ReacTran package written in R [51] and enhanced its biogeochemistry and transport by adding additional chemical reactions and transport properties using the formulation presented in [46, 48]. Resulting model includes dynamics of C, N, O, and S in marine sediments. In addition to these species, model has complex Mn and Fe redox cycles including Mn(II), Mn(III), Fe(II) and Fe(III) as iron oxyhydroxides. Including that much chemical species makes it more realistic however at the expense of increasing computational load to estimate redox dynamics in marine environment. In this setting, with the presence of Mn(III) and Mn(II), manganese becomes an electron shuttle between oxic and anoxic layers. Including soluble Mn(III) besides Mn(II) makes model even more complex since Mn(III) can be either an oxidant or a reductant in different biogeochemical reactions [52].

Main mechanism of this model is composed of partial differential equations which represent mass balance equations for 19 solid and solute species which are listed in Table 2.1. Mass balance of these species include transport processes such as bioturbation, advection(burial) and molecular diffusion. In reaction part, following bio-

geochemical reactions are involved: primary and secondary redox, equilibrium and mineral formation reactions. These mass balance equations are as follows [27, 28]:

$$\frac{\partial C_S}{\partial t} = \frac{1}{\phi_S}\frac{\partial}{\partial x}\left[\underbrace{\phi_S D_b \frac{\partial C_S}{\partial x}}_{Bioturbation} - \underbrace{\phi_S U C_S}_{Advection}\right] + \underbrace{\sum R_S}_{Reactions} \tag{2.1}$$

$$\frac{\partial C_D}{\partial t} = \frac{1}{\phi}\frac{\partial}{\partial x}\left[\underbrace{\phi\left(D_b + \frac{D}{\theta^2}\right)\frac{\partial C_D}{\partial x}}_{Bioturbation+Diffusion} - \underbrace{\phi V C_D}_{Advection}\right] + \underbrace{\sum R_D}_{Reactions} \tag{2.2}$$

where C_s is the mass concentration of a solid per unit volume of solid (mmol L^{-1}), C_d is the mass concentration of a solute per unit volume of pore-water (mmol L^{-1}), t is the time (year), ϕ is the porosity, ϕ_S is the solid fraction of volume (ϕ_S = 1 - ϕ), x is the depth starting from sediment-water interface (cm), D_b is the bioturbation coefficient (cm^2 $year^{-1}$).

2.1.1 Transport processes

In this part, we define transport processes that we derive from [46] which have different parametrization than [30] in some elements of the transport processes. As defined in equations (2.1) and (2.2), transport of species are limited to diffusion, advection(burial) and bioturbation. Therefore, model omits some elements of 1D reactive transport models such as hydrodynamic dispersion, compaction, biological advection, inter-phase mixing of bioturbation and non-local processes such as irrigation.

Porous media includes at least two different phases and their ratio is defined by the term called porosity. Since marine sediments are also a porous media, it is important to include this factor in simulating the transport of species in this kind of environment. Porosity gives the amount of pores -which would be filled with water in marine sediments- divided by the total soil mixture in a certain volume. [53] defined it as the

Table 2.1: Chemical species in the model

Species	Type	Symbol
Redox Species		
Organic carbon	Solid	$C_{org}^{G1}, C_{org}^{G2}$
Oxygen	Solute	O_2
Nitrate	Solute	NO_3^-
Manganese oxide	Solid	MnO_2
Iron oxide	Solid	$Fe(OH)_3$
Sulfate	Solute	SO_4^{2-}
Phosphate	Solute	PO_4
Ammonia & ammonium	Solute	NH_4
Hydrogen Sulfide	Solute	H_2S
Methane	Solute	CH_4
Iron-bound phosphorus	Adsorbed	Fe-P
Metal Ions		
Manganese(II)	Solute	Mn^{2+}
Manganese(III)	Solute	Mn^{3+}
Iron(II)	Solute	Fe^{2+}
Minerals		
Elemental sulfur	Solid	S^0
Iron sulfide	Solid	FeS
Pyrite	Solid	FeS_2
Manganese carbonate	Solid	$MnCO_3$
Iron carbonate	Solid	$FeCO_3$

following:

$$\phi = \frac{\text{volume of interconnected water}}{\text{volume of total sediment or rock}} \tag{2.3}$$

In a quantitative sense, it depends on the depth and assumed to be independent of the time and the porosity function is defined as below [27]:

$$\phi(x) = \phi_\infty + (\phi_0 - \phi_\infty)e^{-\beta x} \tag{2.4}$$

where ϕ_∞ is the porosity at infinite depth, ϕ_0 is the porosity at sediment-water interface and β is the porosity depth attenuation coefficient. In [30], it also defined as the above equation but, we had to add this to the R implementation of the model where porosity was constant throughout the sediment.

While modeling the transport in the sediment, it is important to consider the heterogeneity of the sediments. This heterogeneity is defined as tortuosity and since the diffusion would be disturbed by sediment grains, tortuosity becomes a factor controlling diffusion coefficient. Therefore, diffusion coefficient is defined as the following [27]:

$$D_i = \frac{D_i^0}{\theta^2} \tag{2.5}$$

where D^0 is the diffusion coefficient in particle-free (non-tortuous) solutions and θ is the tortuosity which is defined as $\theta^2 = 1 - \ln(\phi^2)$. Similar equation is included in [30] with a sediment resistivity instead of tortuosity. In R implementation, we added tortuosity as a porosity and depth dependent factor different from R implementation of OMEXDIA.

In this model, an important part of the transport depends on the molecular diffusion. As defined by [27], molecular diffusion is the sum of random motions of individual particles of a matter due to the molecular properties therefore it does not have a velocity component coming from the bulk water movement. In marine environment, diffusion is controlled by Fick's laws of diffusion defined by [54]. According to [27],

Fick's First Law and Fick's Second Law for our sediment model are as follows:

$$\text{Fick's First Law:} \quad J_i = -D_i \phi \frac{\partial C_i}{\partial x}$$

$$\text{Fick's Second Law:} \frac{\partial C_i}{\partial t} = -\frac{1}{\phi}\frac{\partial J_i}{\partial x} = \frac{1}{\phi}\frac{\partial \left(\phi D_i \frac{\partial C_i}{\partial x}\right)}{\partial x}$$

where, J_i is the diffusive flux of i in mass per unit are and time, D_i is the diffusion coefficient of i in area per unit time, C_i is the concentration of i in mass per unit volume, ϕ is the porosity and x is the direction of concentration gradient (in 1D sediment model: depth). Therefore, in Fick's First Law, diffusion coefficient is multiplied by the porosity and the concentration difference along depth gradient to calculate diffusive flux. This calculation is completed by a negative sign because, direction of the concentration gradient and the direction of the flux is opposite. Meaning that, flux is from higher concentration to the lower concentration. Fick's Second Law, gives the total mass exchange as a function of flux multiplied by the total area.

Exact modeling of bioturbation is difficult due to complexity, variety and uncertainty of the ongoing processes. Therefore, bioturbation is also modeled as a diffusive process with a bioturbation rate which is defined as the following [35]:

$$D_b(x) = D_b^0 \exp\left(\frac{x^2}{2\tau_b^2}\right) \tag{2.6}$$

where x is depth, D_b^0 is the bioturbation rate at the sediment-water interface (where x = 0) and τ_b is the half mixing depth of bioturbation. Different from R implementation of OMEXDIA, we added bioturbation also for the dissolved species.

Burial velocity is also a function of depth and can be calculated as in [28]:

$$U(x) = \frac{U_\infty \phi_s(\infty)}{\phi_s(x)} \tag{2.7}$$

$$V(x) = \frac{U_\infty \phi(\infty)}{\phi(x)} \tag{2.8}$$

where $U(x)$ is the solid burial velocity at depth x, U_∞ is the burial velocity at infinite depth, and $V(x)$ is the solute burial velocity at depth x. Depth dependence of burial velocity is also an addition to the R implementation of OMEXDIA.

2.1.2 Redox dynamics

In biogeochemistry side of this model, we aimed to include a full redox ladder and a substantial amounts of secondary reactions to simulate dynamics of sediment with high sensitivity. We combined manganese focus of [46] with the phosphorus oriented [48] to create a model that is capable of calculating depth profiles and fluxes of metals, nutrients and minerals in a anoxic/hypoxic deep sea environment. Range of the reactions included can be seen in Table 2.2.

Table 2.2: Reactions included in the model

Modeled Reactions	Rates
OM Decomposition (OM = $(CH_2O)_A\,(NH_3)_B\,(H_3PO_4)_C$)	
$OM + A\,O_2 \longrightarrow A\,CO_2 + B\,NH_3 + C\,H_3PO_4$	R_{O2}
$OM + \frac{4}{5}\,A\,NO_3^- + \frac{4}{5}\,A\,H^+ \longrightarrow A\,CO_2 + \frac{2}{5}\,A\,N_2 + B\,NH_3 + C\,H_3PO_4$	R_{NO3}
$OM + 2\,A\,MnO_2 + 4\,A\,H^+ \longrightarrow A\,CO_2 + 2\,A\,Mn^{2+} + B\,NH_3 + C\,H_3PO_4$	R_{MnO2}
$OM + 4\,A\,FeOH + 4\,A\rho Fe-P + 8\,A\,H^+ \longrightarrow A\,CO_2 + 4\,A\,Fe^{2+} + B\,NH_3 + (C + 4\,A\rho)\,H_3PO_4$	R_{FeOH}
$OM + \frac{1}{2}\,A\,SO_4^{2-} + A\,H^+ \longrightarrow A\,CO_2 + \frac{1}{2}\,A\,H_2S + B\,NH_3 + C\,H_3PO_4$	R_{SO4}
$OM \longrightarrow \frac{1}{2}\,A\,CO_2 + \frac{1}{2}\,A\,CH_4 + B\,NH_3 + C\,H_3PO_4$	R_{CH4}
Secondary Redox Reactions	
$NH_4^+ + 2\,O_2 \longrightarrow NO_3^- + H_2O + 2\,H^+$	R_{Nitri}
$4\,Mn^{2+} + O_2 + 4\,H^+ \longrightarrow 4\,Mn^{3+} + 2\,H_2O$	R_{MnIIOx}
$4\,Mn^{3+} + 5\,O_2 + 4\,H^+ \longrightarrow 4\,MnO_2 + 2\,H_2O$	$R_{MnIIIOx}$
$4\,Fe^{2+} + O_2 + 8\,HCO_3^- + 2\,H_2O + 4\,\rho H_3PO_4 \longrightarrow 4\,Fe(OH)_3 + 4\,\rho Fe-P + 8\,CO_2$	R_{FeIIOx}
$H_2S + 2\,O_2 \longrightarrow SO_4^{2-} + 2\,H^+$	R_{H2SOx}
$CH_4 + 2\,O_2 \longrightarrow CO_2 + 2\,H_2O$	R_{CH4Ox}
$FeS + 2\,O_2 \longrightarrow Fe^{2+} + SO_4^{2-}$	R_{FeSOx}
$2\,FeS_2 + 7\,O_2 + H_2O \longrightarrow 4\,SO_4^{2-} + 2\,Fe^{2+} + 2\,H^+$	R_{FeS2Ox}
$2\,Fe^{2+} + MnO_2 + 2\,H_2O + 2\,HCO_3^- + 2\,\rho H_3PO_4 \longrightarrow Mn^{2+} + 2\,Fe(OH)_3 + 2\,\rho Fe-P + 2\,CO_2$	$R_{FeIIMnO2x}$
$Fe^{2+} + Mn^{3+} + 3\,OH^- + \rho H_3PO_4 \longrightarrow Mn^{2+} + Fe(OH)_3 + \rho Fe-P$	$R_{FeIIMnIIIx}$

Table 2.2: Continued

Modeled Reactions	Rates
$H_2S + MnO_2 + 2\,H^+ \longrightarrow S^0 + Mn^{2+} + 2\,H_2O$	$R_{H2SMnO2x}$
$H_2S + 2\,Mn^{3+} \longrightarrow S^0 + 2\,Mn^{2+} + 2\,H^+$	$R_{H2SMnIIIx}$
$H_2S + 2\,Fe(OH)_3 + 2\,\rho Fe-P + 4\,H^+ \longrightarrow 2\,Fe^{2+} + S^0 + 6\,H_2O + 2\,\rho H_3PO_4$	$R_{H2SFeOHx}$
$5\,Mn^{2+} + 2\,NO_3{}^- + 4\,H_2O \longrightarrow 5\,MnO_2 + N_2 + 8\,H^+$	$R_{MnIINO3x}$
$NO_3{}^- + H_2S + H_2O \longrightarrow SO_4{}^{2-} + NH_4{}^+$	$R_{NO3H2Sx}$
$4\,S^0 + 4\,H_2O \longrightarrow 3\,H_2S + SO_4{}^{2-} + 2\,H^+$	R_{S0x}
$CH_4 + SO_4{}^{2-} + CO_2 \longrightarrow H_2S + 2\,HCO_3{}^-$	$R_{CH4SO4x}$
Mineral Formation Reactions	
$Fe^{2+} + H_2S \longleftrightarrow FeS + 2\,H^+$	$R_{FeIIH2Sx}$
	$R_{FeSDiss}$
$FeS + H_2S \longrightarrow FeS_2 + H_2$	$R_{FeSH2Sx}$
$Fe^{2+} + CO_3{}^{2-} \longleftrightarrow FeCO_3$	$R_{FeIICO3x}$
	$R_{FeCO3Diss}$
$Mn^{2+} + CO_3{}^{2-} \longleftrightarrow MnCO_3$	$R_{MnIICO3x}$
	$R_{MnCO3Diss}$
*ρ = adsorption rate for phosphate	

In this model, organic matter is pooled into two types according to their reactivity: highly reactive (OM_1) and less reactive organic matter (OM_2). Both types of organic matter are remineralized depending on the thermodynamic ladder of electron acceptors which is based on free energy yield of reactions [42]. To model this mechanism quantitatively, Monod kinetics is used where reduction of lower energy yielding oxidants is inhibited by the availability of greater energy yielding oxidants which leads to sequential use of electron acceptors from the most to the least energy yielding one (Table 2.3). Model includes reduction of oxygen, nitrate, manganese oxide, iron oxide and sulfate. In addition to these, as a last step methanogenesis is also included in the model. However in OMEXDIA, manganese oxide, iron oxide, sulfate reductions and methanogenesis are represented by one reaction which produces oxygen demanding units (ODU) [30].

Table 2.3: Reaction rate expressions for primary redox reactions

R_{O_2}	$= \sum_i k_i C^i_{org} \left(\frac{[O_2]}{k_{O_2} + [O_2]}\right)$
R_{NO_3}	$= \sum_i k_i C^i_{org} \left(\frac{[NO_3]}{k_{NO_3} + [NO_3]}\right) \left(\frac{k^{inh}_{O_2}}{k^{inh}_{O_2} + [O_2]}\right)$
R_{MnO_2}	$= \sum_i k_i C^i_{org} \left(\frac{[MnO_2]}{k_{MnO_2} + [MnO_2]}\right) \left(\frac{k^{inh}_{NO_3}}{k^{inh}_{NO_3} + [NO_3]}\right) \left(\frac{k^{inh}_{O_2}}{k^{inh}_{O_2} + [O_2]}\right)$
R_{FeOH_3}	$= \sum_i k_i C^i_{org} \left(\frac{[FeOH_3]}{k_{FeOH_3} + [FeOH_3]}\right) \left(\frac{k^{inh}_{MnO_2}}{k^{inh}_{MnO_2} + [MnO_2]}\right) \left(\frac{k^{inh}_{NO_3}}{k^{inh}_{NO_3} + [NO_3]}\right) \left(\frac{k^{inh}_{O_2}}{k^{inh}_{O_2} + [O_2]}\right)$
R_{SO_4}	$= \psi \sum_i k_i C^i_{org} \left(\frac{[SO_4]}{k_{SO_4} + [SO_4]}\right) \left(\frac{k^{inh}_{FeOH_3}}{k^{inh}_{FeOH_3} + [FeOH_3]}\right) \left(\frac{k^{inh}_{MnO_2}}{k^{inh}_{MnO_2} + [MnO_2]}\right) \left(\frac{k^{inh}_{NO_3}}{k^{inh}_{NO_3} + [NO_3]}\right) \left(\frac{k^{inh}_{O_2}}{k^{inh}_{O_2} + [O_2]}\right)$
R_{CH_4}	$= \psi \sum_i k_i C^i_{org} \left(\frac{[CH_4]}{k_{CH_4} + [CH_4]}\right) \left(\frac{k^{inh}_{SO_4}}{k^{inh}_{SO_4} + [SO_4]}\right) \left(\frac{k^{inh}_{FeOH_3}}{k^{inh}_{FeOH_3} + [FeOH_3]}\right) \left(\frac{k^{inh}_{MnO_2}}{k^{inh}_{MnO_2} + [MnO_2]}\right) \left(\frac{k^{inh}_{NO_3}}{k^{inh}_{NO_3} + [NO_3]}\right) \left(\frac{k^{inh}_{O_2}}{k^{inh}_{O_2} + [O_2]}\right)$

*ψ is the attenuation factor controlling SO_4 reduction and methanogenesis

** $k_i C^i_{org}$ = (reactivity)(Availability) of OM i where $i \in$ {OM1,OM2}

Apart from primary redox reactions, model also includes secondary redox reactions as defined in [35] and [31]. In the model, these reactions are treated as second order reactions and with kinetic rate = k[reductant][oxidant]. In these reactions, we focused especially on metals and hydrogen sulfide to correctly simulate sulfidic/suboxic zones. Additionally, anaerobic oxidation of methane is also considered since it is a crucial process controlling methane exchange between sediment and water column.

In addition to secondary redox reactions, model includes reversible mineral formation reactions for $FeCO_3$, $MnCO_3$, FeS and FeS_2 which are modeled as second order with increased solvability to focus more on flux experiments. Carbonate is also included as carbonate based minerals which is important for metal cycling and also carbonate ion is crucial to some organisms such as cocolithophores, foraminefera, mussels and corals [6].

Adsorption of phosphate and ammonium are also included in this model study. Adsorption of ammonium is modeled with a fixed ratio as in [30, 55] however, for phosphate, adsorption to iron oxides is considered with a similar approach in [47, 48, 56].

In this framework, we included phosphate to be converted into iron-bound phosphate with a ratio in reactions where iron oxides are produced.

Table 2.4: Reaction rate expressions for secondary redox and mineral formation reactions

Secondary Redox Reactions	
R_{Nitri}	$= k_{nitri}[NH_4][O_2]$
R_{MnIIOx}	$= k_{MnIIox}[Mn^{2+}][O_2]$
$R_{MnIIIOx}$	$= k_{MnIIIox}[Mn^{3+}][O_2]$
R_{FeIIOx}	$= k_{FeIIox}[Fe^{2+}][O_2]$
R_{H2SOx}	$= k_{H2Sox}[H_2S][O_2]$
R_{CH4Ox}	$= k_{CH4ox}[CH_4][O_2]$
R_{FeSOx}	$= k_{FeSox}[FeS][O_2]$
R_{FeS_2Ox}	$= k_{FeS2ox}[FeS_2][O_2]$
$R_{FeIIMnO2x}$	$= k_{FeIIMnO2x}[Fe^{2+}][MnO_2]$
$R_{FeIIMnIIIx}$	$= k_{FeIIMnIIIx}[Fe^{2+}][Mn^{3+}]$
$R_{H2SMnO2x}$	$= k_{H2SMnO2x}[H_2S][MnO_2]$
$R_{H2SMnIIIx}$	$= k_{H2SMnIIIx}[H_2S][Mn^{3+}]$
$R_{H2SFeOHx}$	$= k_{H2SFeOHx}[H_2S][FeOH_3]$
$R_{MnIINO3x}$	$= k_{MnIINO3x}[Mn^{2+}][NO_3]$
$R_{H2SNO3x}$	$= k_{H2SNO3x}[H_2S][NO_3]$
R_{S0x}	$= k_{S0x}[S^0]$
$R_{CH4SO4x}$	$= k_{CH4SO4x}[CH_4][SO_4]$
Mineral Formation Reactions	
$R_{FeIIH2Sx}$	$= k_{FeIIH2Sx}[Fe^{2+}][H_2S]$
$R_{FeSdiss}$	$= k_{FeSdiss}[FeS]$
$R_{FeIICO3x}$	$= k_{FeIICO3x}[Fe^{2+}][CO_3]$
$R_{FeCO3diss}$	$= k_{FeCO3diss}[FeCO_3]$
$R_{MnIICO3x}$	$= k_{MnIICO3x}[Mn^{2+}][CO_3]$
$R_{MnCO3diss}$	$= k_{MnCO3diss}[MnCO_3]$

2.1.3 Boundary Conditions

For simplification of the model, it is designed as uncoupled from water column. In this context, model requires concentrations of solutes and fluxes of solids at the sediment-water interface. In this regard, we use data from the literature to simulate the Black Sea sulfidic and suboxic conditions. As the bottom boundary condition, the model considers a no-gradient boundary condition where concentration gradient is equal to zero with increasing depth.

2.1.4 Solution of the Model

This model is written in R where we construct initial conditions, boundary conditions, transport properties, biogeochemical reactions, and additional parameters. Then, this parameter set is passed to ReacTran package [51] to construct the governing partial differential equations. When the set of partial differential equations are constructed, they are converted to ordinary differential equations using numerical differencing. Lastly, the resulting expressions are solved using ODE solvers from the literature. In our case, we use LSODE ODE solver [57] which is made available by R package deSolve in R [58].

CHAPTER 3

RESULTS AND DISCUSSION

In this chapter, we present our simulation results for the Black Sea. First, we start with depth profiles calculated through a 50cm depth of the sediment. Secondly, we focus on mineralization rates to quantify importance of different redox pathways. Then, in the light of these depth profiles, we calculate flux estimations through the water column to be able to investigate impact of benthic fluxes. Additionally, we take a closer look at the P cycle by focusing on sources of the P flux (OM, adsorbed). Finally, we upscale our results to be able to compare impact of benthic fluxes with other nutrient resources in a broader scale by using data of Marmara Sea retrieved from calculations of MARMOD Project.

3.1 Parameter Selection for the Diagenetic Model

In our simulations, we considered several sources for parameters of our model. Since our main focus is the Black Sea, we tried to collect data from the literature that are directly related to the Black Sea or similar environments. Most of the data comes from our main focus [46] and the rest is completed by [55] because of its Black Sea focus and [48, 47] to be able to include adsorption of phosphate. Range of our corresponding parameter values from these studies can be seen in Table A.1.

3.2 Simulations with changing levels of O_2

In the simulations of the thesis, aim was to observe effects of bottom water O_2 concentrations on sediment biogeochemistry and subsequent feedbacks to the water column. Therefore, in our experiments, we tested 5 different O_2 levels: 295, 140, 80, 40 and 5 μM of O_2. By doing this, we included O_2 levels from saturation concentrations to the fully anoxic conditions. In doing this, we ignored the long-term oscillations on O_2 concentrations due to changes in climatic and environmental conditions.

The accumulation of H_2S is another critical component in determining the benthic biogeochemical fluxes as sulfide is a strong binding ligand for metals as well as it can be a powerful reducing agent for O_2 and oxidized forms of metals. Hence, along with O_2 variation, the development of benthic anoxia was also tested under three different scenarios: sulfidic (>200m), mildly sulfidic (~100m) and suboxic (65-100m) [59]. By doing this, sediment biogeochemistry under several conditions that exist in the Black Sea and that may currently be developing in the Marmara Sea are investigated.

3.2.1 Scenario 1: Sulfidic Sediment Biogeochemistry

Results of our simulations for the highly sulfidic conditions can be seen in Figure 3.1. From this figure, it was found that the general mechanics of the model works as expected for all scenarios which serve as a verification of the newly developed biogeochemical model. Overall, the expected redox sequence of electron acceptors was successfully simulated in all three scenarios, which allow for recognizing major patterns in benthic fluxes.

These simulations showed that the decrease of O_2 triggers denitrification (nitrate reduction) and anoxic mineralization of the organic matter gradually. Until the depletion of O_2, nitrification (ammonium oxidation to nitrate) takes place therefore, NO_3

concentrations increase for a short time, however, after O_2 concentrations decrease, NO_3 consumption increases which leads to ammonia production and accumulation in the sediment. After the NO_3, MnO_2 is the next favorable oxidant therefore, MnO_2 is also depleted very quickly. As a result of MnO_2 reduction, Mn^{2+}, Mn^{3+} and $MnCO_3$ concentrations increase downcore. Since the model has a complex manganese cycle, increase of Mn^{2+} after depletion of MnO_2 can be attributed to reactions of Mn^{3+} with Fe(II) and hydrogen sulfide; and dissolution of produced $MnCO_3$. $Fe(OH)_3$ reduction starts when MnO_2 reach lower concentrations. Product of this process is Fe(II) which has a potential to stay in ion form or accumulate as FeS, FeS_2 or $FeCO_3$. After $Fe(OH)_3$ reduction, SO_4 reduction continues along with the anaerobic oxidation of CH_4 (AOM) which depletes SO_4 in about 10 centimeters. Depletion of SO_4 is relatively slower than the other oxidants because of high reproduction of SO_4 through oxidation of hydrogen sulfide with O_2 and NO_3, oxidation of pyrite and reaction between sulfur and water. Although, recycling of sulfur is complex, eventually with the low availability of oxidants, it accumulates as H_2S as expected. When H_2S increases, it reacts with Mn^{3+}, MnO_2 and $Fe(OH)_3$ to form S^0 in few centimeters where metal oxides are present. In absence of any other oxidants, methanogenesis dominates the environment and CH_4 concentrations increase with increasing depth. In terms of phosphate, in first 2 centimeters where $Fe(OH)_3$ reduction occurs, gradient in phosphate production is steeper compared to the deeper layer with no $Fe(OH)_3$. This is due to release of adsorbed iron-bound phosphate while $Fe(OH)_3$ reduction.

As can be seen above, the model gives reasonable representation of the mechanism of the sediment biogeochemistry. In the remaining part, the model's sensitivity to O_2 is tested to acquire important implications on sediment biogeochemistry.

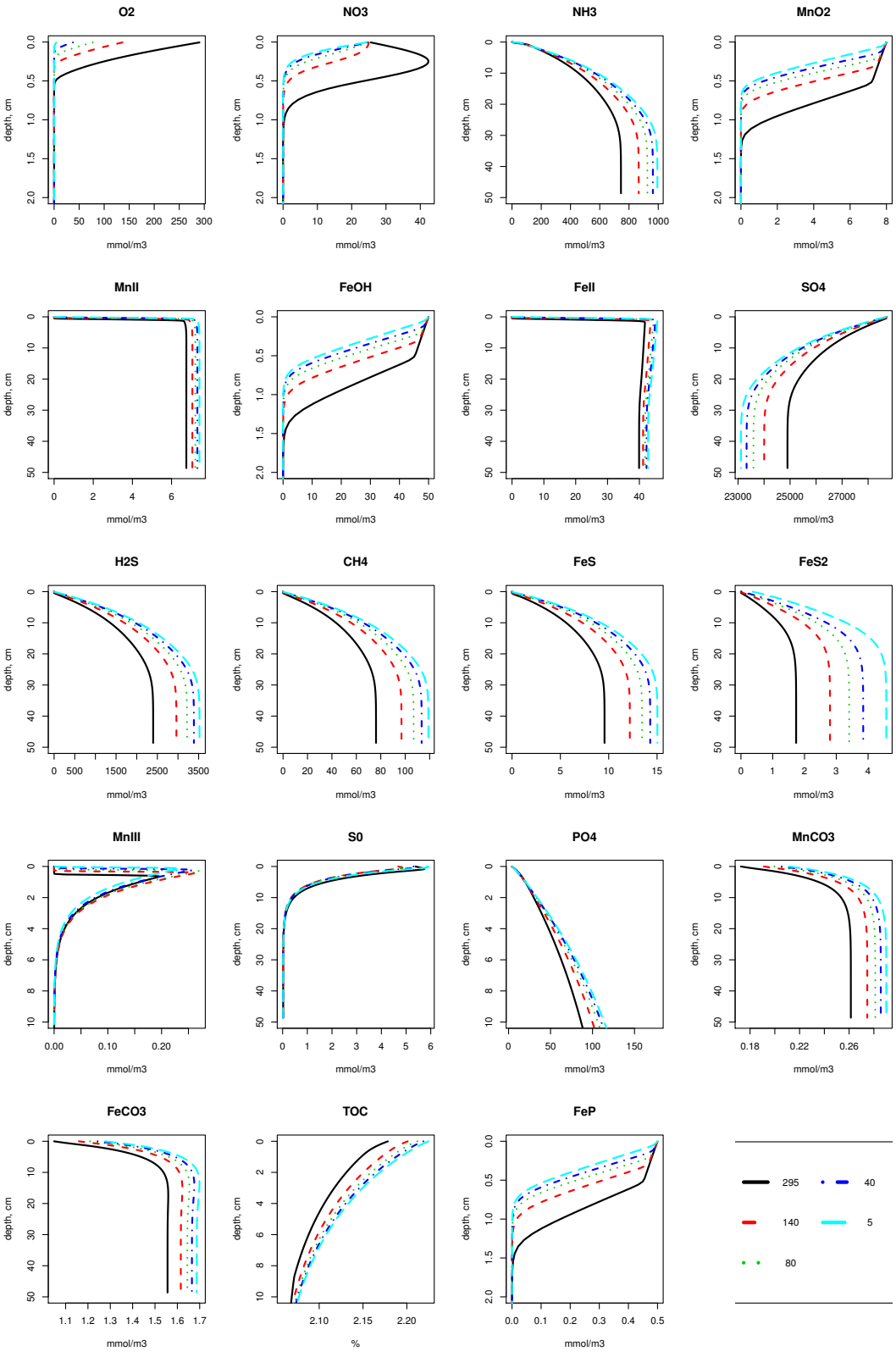

Figure 3.1: Model Results for Changing Levels of O_2 (μM) - Sulfidic

In different O_2 levels, significant shifts in the patterns of the sediment biogeochemistry are observed. First thing to notice is the decrease in the downcore accumulation of NO_3, $Fe(OH)_3$, MnO_2 and SO_4 therefore, steeper concentration profiles when O_2 is lower due to faster consumption and lower recycling. In terms of Fe^{2+} and Mn^{2+} concentrations, the faster consumption of $Fe(OH)_3$ and MnO_2 causes metal ion concentrations to increase in shallower depths (near the sediment surface, near seafloor) than more oxygenated conditions. Additionally, since the system has very abundant SO_4, it produces high amounts of H_2S with reduction of SO_4 or anaerobic oxidation of methane. In abundance of SO_4, due to presence of anaerobic oxidation of methane, CH_4 concentrations are lower compared to other species that are produced by the decomposition of organic matter such as PO_4 and NH_4 even if we expect more due to the OM stoichiometry that we use (106:18:1). In between 30-40 centimeters where OM is depleted, SO_4 concentrations are lower and CH_4 concentrations are higher under lower oxygenated conditions as expected. Results also show that, FeS and FeS_2 are produced faster in low-oxygen conditions this is because of the faster release of Fe^{2+} with $Fe(OH)_3$ reduction. Mn^{3+} concentrations depends on Mn^{2+} oxidation therefore, after O_2 is depleted Mn^{3+} concentrations begin to decrease to form $MnCO_3$. Under hypoxic conditions (5μM O_2), Mn^{3+} increase is steeper but for shorter duration due to depletion of O_2. In S^0, due to more available $Fe(OH)_3$ and MnO_2, under oxygenated conditions, S^0 concentrations are slightly more throughout the sediment column. In PO_4 concentrations, we cannot observe impact of release of adsorbed PO_4, this may due to the high amounts of OM mineralization which produces PO_4 in a higher scale. Fe-P graph shows that all iron-bound phosphorus (with the adsorption rate 1%) is released in few centimeters due to the reduction of $Fe(OH)_3$. Similar to [48], decrease in O_2, slows down the potential Fe-P burial. In next section, we aim to observe this effect under suboxic conditions. Similar to FeS and FeS_2, $FeCO_3$ and $MnCO_3$ accumulate faster under low-oxygen conditions due to availability of metal ions to react with CO_3^- ion. Total organic carbon (TOC) decreases rapidly in few centimeters due to the abundance of oxidants.

3.2.2 Scenario 2: Mildly Sulfidic Sediment Biogeochemistry

Results for the mildly sulfidic (but still not strictly suboxic) conditions are presented in the Figure 3.2. Under these conditions, O_2 and NO_3 concentrations remain the same however since the rates of SO_4 reduction and methanogenesis is decreased, ammonia output due to OM decomposition is lower compared to the previous case. Metal cycles also remains closer to the previous case with a slight increase in reduction rates of metal oxides however, FeS and FeS_2 formation reactions are slower due to significantly lower H_2S production. Similar to this impact, change in H_2S production decreased S^0 concentrations. However, carbonate took advantage of slightly increased metal ions to form more $FeCO_3$ and $MnCO_3$ since they are independent from sulfur cycle. Different from previous simulation, since there is less overall PO_4 release to sediment pore-waters due to lower OM mineralization, PO_4 concentrations are able to show a steeper gradient caused by the adsorbed PO_4 release from $Fe(OH)_3$ reduction despite the similar looking Fe-P curve. In this simulation, a flatter TOC curve with higher values was observed which supports the above implications of lower rates of OM mineralization.

Compared to the fully sulfidic simulation the mildly sulfidic scenario displayed more sensitivity to the variations in the bottom water O_2 levels. For example, maximum ammonium accumulation at 50 cm depth decreased to 110 μM to nearly 70 μM, corresponding to almost 50% decrease. Conversely, hydrogen sulfide maximum increased threefold from nearly 40 μM to 120 μM, also reflected as increase in sulfide gradients. Solid state metal oxide inventories (Fe and Mn oxides) also decrease with decreasing O_2 levels, indicating the mildly sulfidic but hypoxic conditions significantly yielding in the reduction of the solid metal pools and their transfer to dissolved phases and /or other solid pools such as carbonates. These findings, overall supports the central hypothesis of this thesis that hypoxic conditions induce metal mobilization and trigger a series of complex feedbacks on N and P cycles.

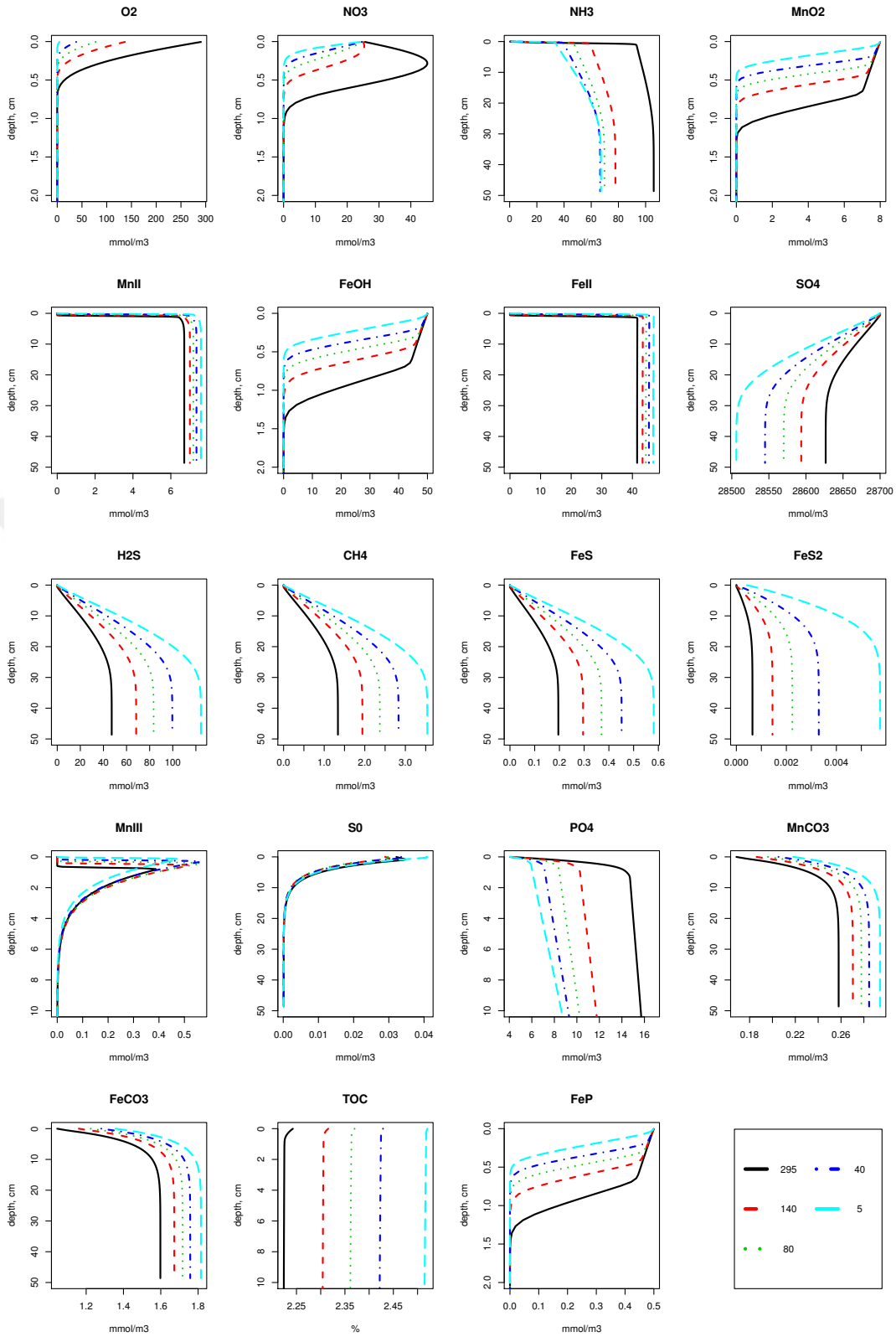

Figure 3.2: Model Results for Changing Levels of O_2 (μM) - Mildly Sulfidic

In order to compare these results to the total absence of sulfide and methane in sediment porewaters, the organic matter degradation through the final two steps has been minimized and the simulations in the next section have been generated.

3.2.3 Scenario 3: Strictly Suboxic Sediment Biogeochemistry

In addition to mildly sulfidic scenario, a strictly suboxic scenario - which is important in the case of the Black Sea- is also tested to see potential response of the system under absence of the two of the redox pathways.

In strictly suboxic scenario, depth profiles are similar to the mildly sulfidic conditions however, SO_4 reduction and methanogenesis are zero. Therefore, there is no production of H_2S and CH_4 which also leads to inhibition of sulfur dependent mineral formations such as FeS and FeS_2. Eventually, metals are kept in their ion forms but a significant fraction of metals have been mobilized due to suboxic conditions and transferred to the carbonate phases. As will be elaborated later in the flux discussion, in this scenario only the fluxes of metals to the bottom waters are also induced. Notably, at the lower end of the O_2 levels efflux of Mn to the bottom water starts. Similar to the previous two scenarios, the sediment column turns to being a sink for NO_3 with decreasing O_2 levels. In conjunction with the previous scenarios, these results well establish that the hypoxia triggers denitrification and NO_3 intake into the sediment. Due to denitrification reaction, NO_3 is reduced to N_2 gas and effuses out.

In some of the depth profiles such as H_2S, CH_4, FeS and S^0 due to the nature of the computational studies, we see fluctuations. These fluctuations are always present in our simulations due to the limitations on numerical accuracy but in this case, they are observable because some of the state variables are forced strictly to zero. Since the scales are very low therefore, they are ignorable.

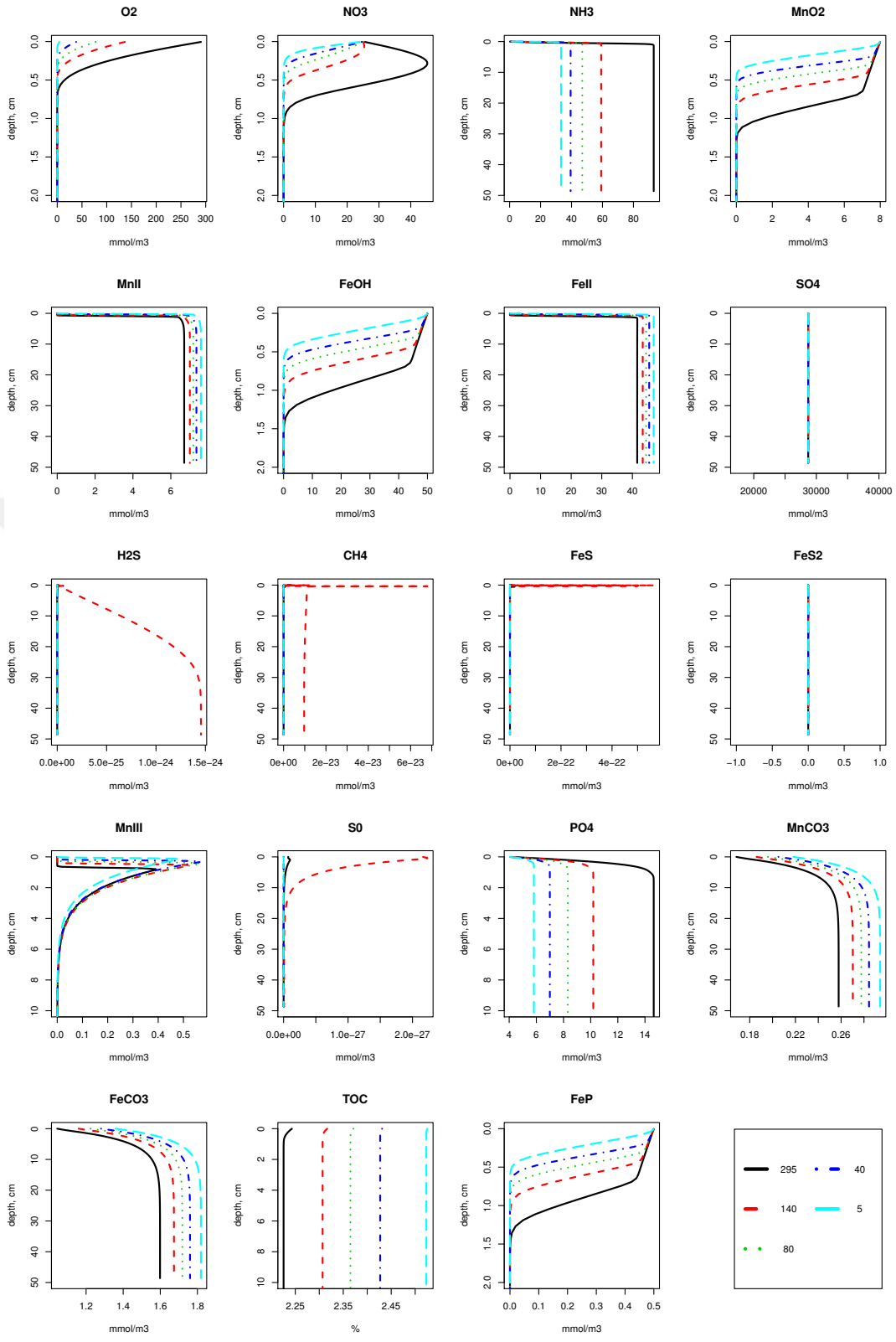

Figure 3.3: Model Results for Changing Levels of O_2 (μM) - Strictly Suboxic

3.3 Discussion

To validate our model, we used data from [60] which included species such as iron, manganese, sulfur and pyrite. In dataset, we interpolated the missing data points using the rest of the data. R-squared statistics that we got were not perfect but, they can be increased with proper calibration of initial conditions to the exact study site. Since our model is combination of several approaches, it was difficult to determine parameters especially for a unique system like the Black Sea. Our initial validation effort using R-squared statistics gave the following values: iron (63.2%), manganese (25.6%), sulfur (76.6%) and pyrite (85.5%). Especially manganese is critical and this can be due to the complexity in manganese cycle that we include in our model.

To gain general insights, we discuss outcome of our simulations in terms of their potential impacts on broader scales starting with the water column. In this regard, first the mineralization rates and fluxes to the bottom water are investigated. In doing this, the aim is to quantify the changes occurring under changing levels of O_2 concentrations which have potential to affect marine ecosystem. Additionally, we focus specifically on P-cycle since it is a limiting nutrient in production of OM in the water column. Finally, we aim to derive broader-scale implications from our simulation results to be able to prove the role and importance of sediment biogeochemistry of coastal, eutrophied marine ecosystems which comprise an important carbon cycle venue in the Earth System.

3.3.1 OM Degradation Pathways

In this section, percentages of OM pathways are analyzed to get a better understanding of ongoing redox dynamics in the sediment under changing O_2 levels.

In Figure 3.4, under sulfidic conditions, oxic mineralization is the primary pathway

for OM degradation when O_2 is available. As O_2 concentrations decrease, denitrification and SO_4 reduction rates increase. In the lowest-oxygen scenario, denitrification is performed as a secondary redox pathway and takes the largest portion of OM mineralization as expected. However, due to their limiting supply from the bottom water, $Fe(OH)_3$ and MnO_2 reductions do not take large portions and they are inhibited by the availability of NO_3. When NO_3 is depleted, lower concentrations of $Fe(OH)_3$ and MnO_2 did not suffice enough to inhibit reduction of SO_4 which has a relatively larger initial concentration. Therefore, it takes second largest portion of OM mineralization in the absence of O_2. This redox pattern align well with [61] which focuses on redox cycle in suboxic-anoxic interface zone of the Black Sea. Additionally, due to abundance of SO_4, it has a large inhibition term for methanogenesis leading to less amounts of methanogenesis compared to the rest of the mineralization pathways.

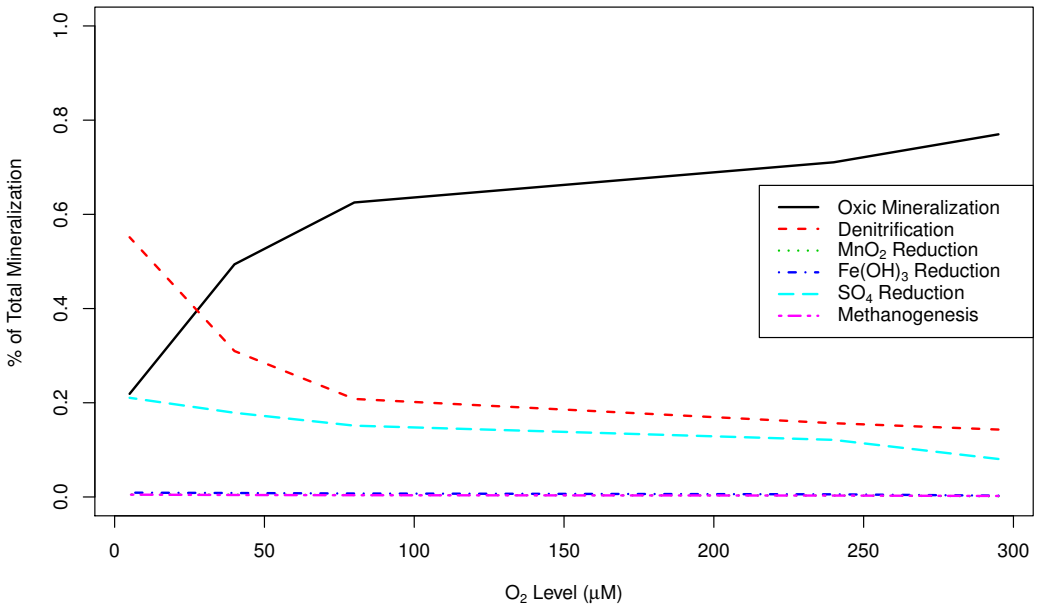

Figure 3.4: Distribution of Mineralization Pathways Under Sulfidic Conditions

When SO_4 reduction and methanogenesis rates are decreased, it was observed that oxic mineralization takes higher percentage in total OM degradation as in Figure 3.5.

Under these conditions, decrease in O_2 is tolerated mainly by denitrification. Compared to previous simulation, portion of denitrification more rapidly increases with decreasing O_2 taking up the part mineralized by SO_4. Additionally, $Fe(OH)_3$ and MnO_2 reductions are also slightly increased compared to previous conditions. At the same time, because of the increase in oxic mineralization, resupply of NO_3, $Fe(OH)_3$ and MnO_2 decrease.

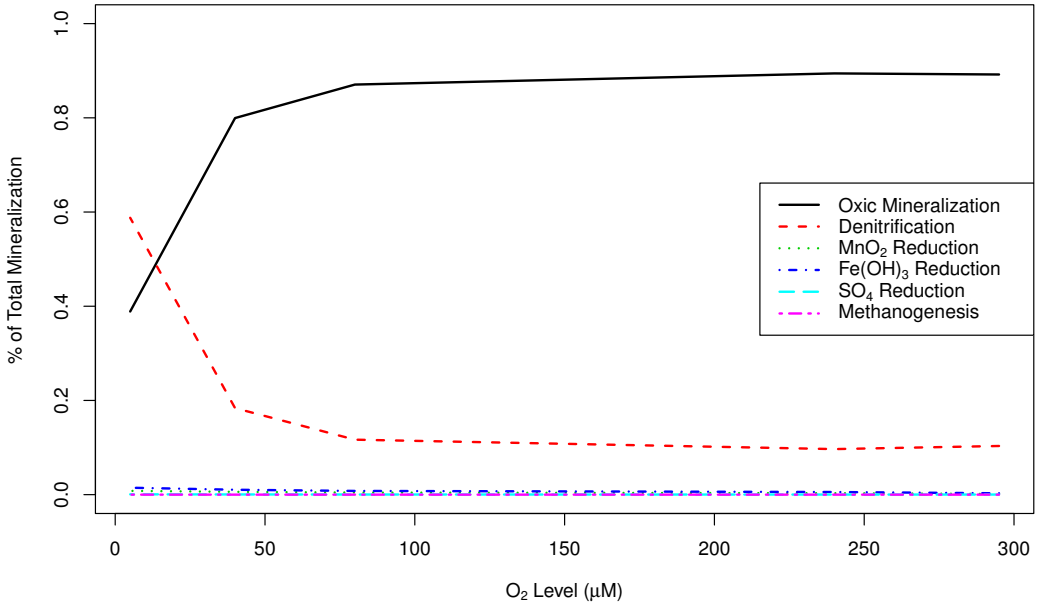

Figure 3.5: Distribution of Mineralization Pathways Under Mildly Sulfidic Conditions

Under strictly suboxic conditions, SO_4 reduction and methanogenesis are zero therefore, rest of the OM mineralization pathways are pushed more as can be seen in Figure 3.6. Since this scenario is very similar to the previous one, figures might not show enough differences to prove effect of strictly suboxic conditions. In the following parts we will be focusing more on the differences between these scenarios in terms of fluxes under changing level of O_2.

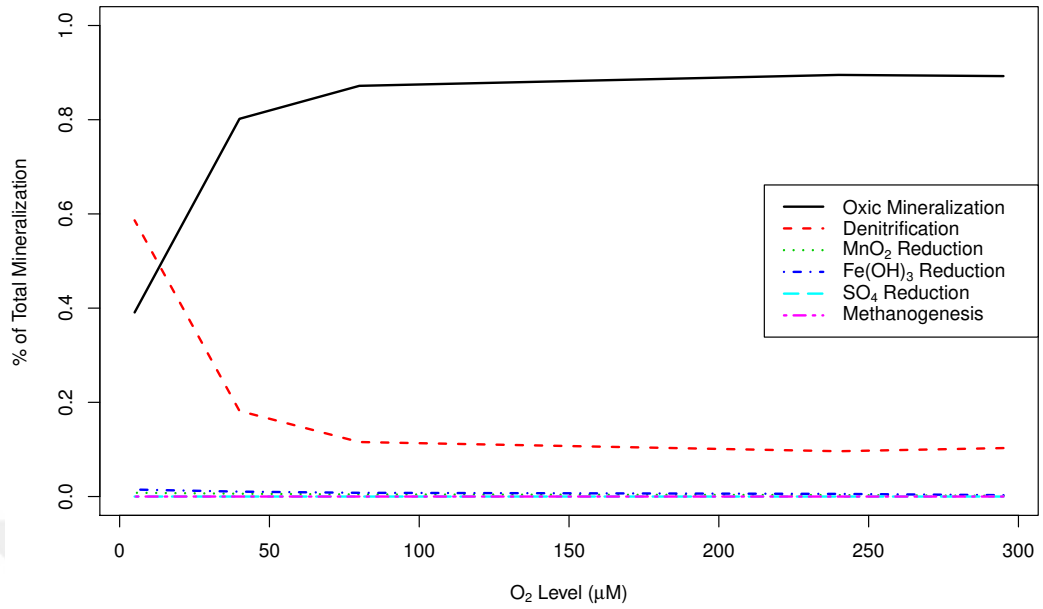

Figure 3.6: Distribution of Mineralization Pathways Under Suboxic Conditions

3.3.2 Estimations on Fluxes to the Water Column

Life and production in the water column is promoted by nutrient inputs from surrounding environments such as land, atmosphere and sediments. Land inputs are transferred via rivers which deliver nutrients and anthropogenic pollutants to the oceans. In terms of our focus the Black Sea, there are substantial amount of N and P inputs to the water column through the Danube River (599 kg NO_3-N $km^{-2}yr^{-1}$, 24 PO_4-P $km^{-2}yr^{-1}$) [62]. The Black Sea also a deposit site for redox sensitive metals such as Fe and Mn through the Danube River and a set of Turkish Rivers [63]. Atmospheric fluxes can be in bulk or wet form which supplies atmospheric particles into the water column. According to [64], the Black Sea has atmospheric nutrient input of around 600 kg N $km^{-2}yr^{-1}$ and 100 kg P $km^{-2}yr^{-1}$ for bulk deposition and 300 kg N $km^{-2}yr^{-1}$ and 30 kg P $km^{-2}yr^{-1}$ for wet deposition. In this part, we aim to study importance of benthic fluxes along with these other sources.

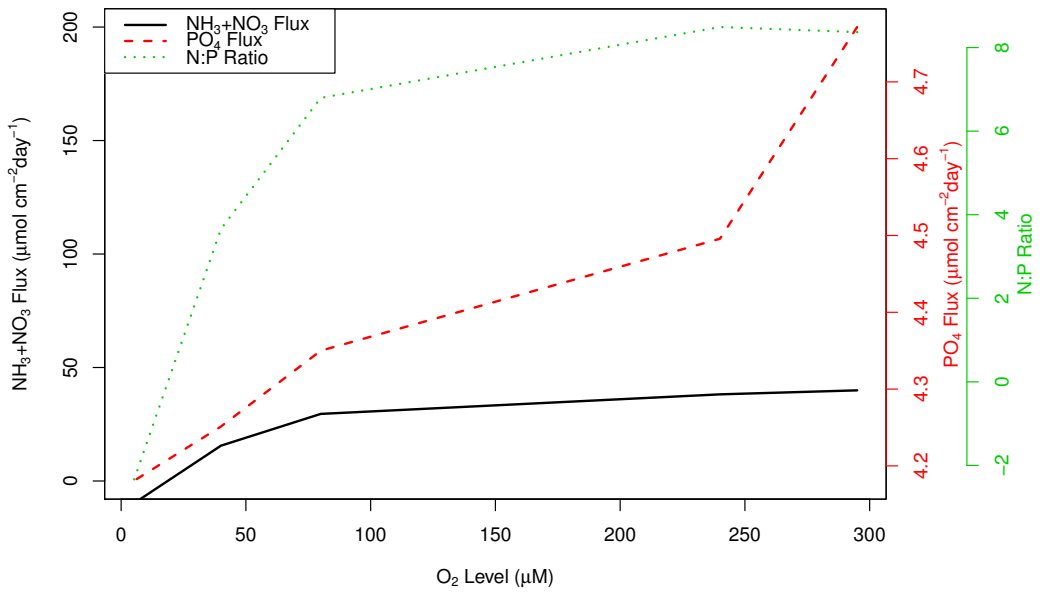

Figure 3.7: NH_3 and PO_4 Fluxes Under Sulfidic Conditions

Sediment to bottom-water fluxes are crucial for the marine biogeochemistry since they have a potential to affect marine life. Under hypoxia, nutrients such as ammonia and phosphate are the main fluxes from sediments to the water column which have a potential to stimulate primary production [17]. In this section, we investigate changes in fluxes under varying levels of O_2 concentration. In the following tables and figures fluxes are demonstrated in μmol cm^{-2}day^{-1} units. Negative values in tables means that fluxes are from sediment to the water column. Positive values stand for the sediment uptake from water column.

Under sulfidic conditions, flux of some species increase critically such as H_2S as seen in Table 3.1. Due to the high supply of H_2S, iron is kept in mineral forms therefore, we do not observe iron fluxes. NH_3 is also increasing with the decreasing O_2 even with less OM mineralization. This is because of the less nitrification process with lower O_2. Additionally, NO_3 fluxes decrease and eventually turn over into intake due to high consumption under absence of O_2. Besides, when O_2 is critically low, sed-

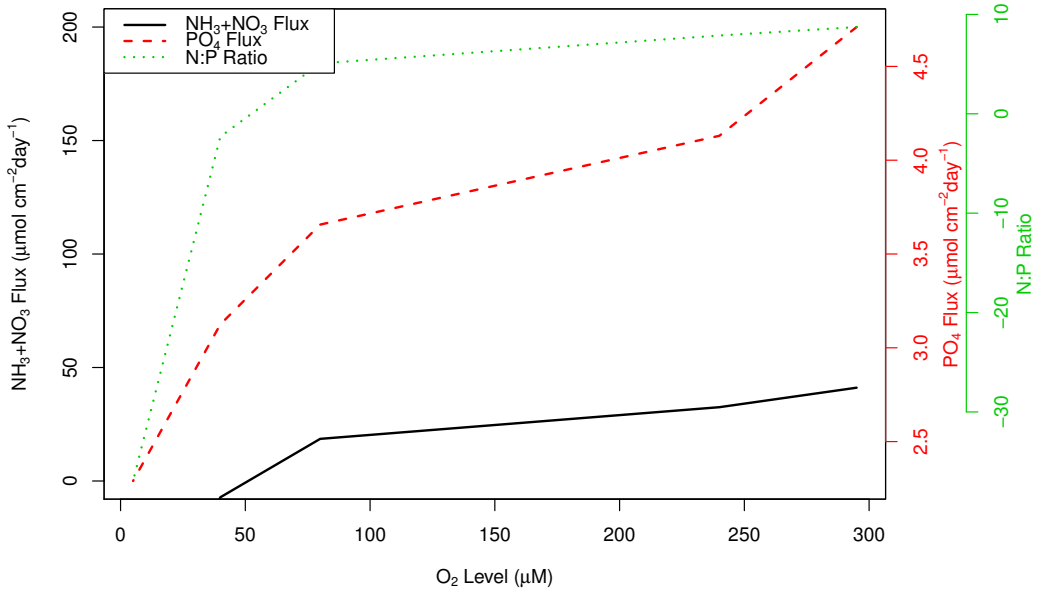

Figure 3.8: NH_3 and PO_4 Fluxes Under Mildly Sulfidic Conditions

iment starts to release manganese ions to the bottom water. PO_4 fluxes are seem to decrease with lower OM mineralization due to less oxic mineralization. Therefore, we can say that it is mainly based on the OM mineralization rather than release of adsorbed PO_4 as also presented in [48]. A detailed discussion on effect of adsorption on PO_4 cycle is presented in the following section.

When SO_4 reduction and methanogenesis is decreased, overall OM degradation decreases due to limited availability as in Table 3.2. Therefore, PO_4 and NH_3 fluxes are less under mildly sulfidic conditions but with decreasing O_2, NH_3 fluxes still increase due to the same mechanism described in the previous scenario. Along with the decrease in SO_4 reduction, H_2S fluxes decrease in substantial amounts. Since this condition forces denitrification, NO_3 intake fluxes also increase due to scarcity of O_2. Apart from these, slight increase in manganese ion fluxes are also observed.

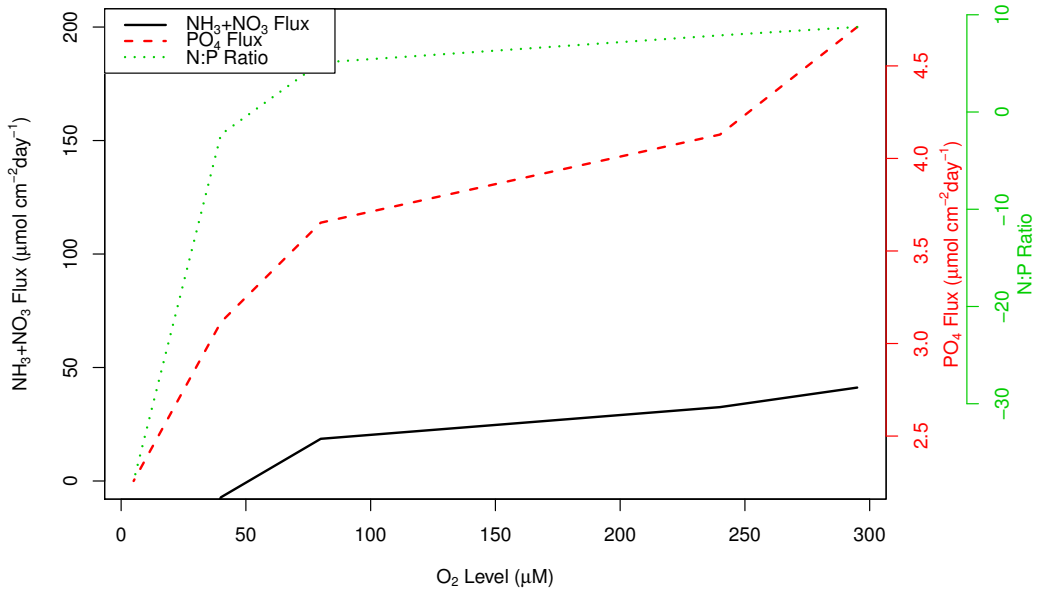

Figure 3.9: NH_3 and PO_4 Fluxes Under Suboxic Conditions

Table 3.2: Mineralization Rates and Flux Estimates for Mildly Sulfidic Conditions

BW O_2 (μM)	Oxic Min.	Denit.	MnO_2 Red.	$Fe(OH)_3$ Red.	SO_4 Red.	CH_4	PO_4 flux	NH_3 flux	NO_3 flux	H_2S flux	Mn^{2+} flux	Mn^{3+} flux	Fe^{2+} flux
295	89.20%	10.33%	0.15%	0.29%	0.02%	0.00%	-4.65	-16.93	-24.16	0.000	0.000	0.000	0.000
240	89.43%	9.67%	0.31%	0.56%	0.02%	0.00%	-4.09	-44.57	12.05	0.000	0.000	0.000	0.000
80	87.06%	11.67%	0.45%	0.79%	0.03%	0.00%	-3.64	-56.41	37.85	0.000	0.000	0.000	0.000
40	79.95%	18.37%	0.60%	1.04%	0.04%	0.00%	-3.12	-55.88	63.06	-0.018	0.000	0.000	0.000
5	38.88%	58.78%	0.80%	1.47%	0.07%	0.00%	-2.29	-42.7	127.31	-2.027	-0.028	-0.081	0.000

Different from mildly sulfidic conditions, under strictly suboxic conditions, SO_4 reduction and methanogenesis is not available therefore, H_2S fluxes are zero (see Table 3.3). However, this change from mildly sulfidic to suboxic conditions did not affect the rest of fluxes considerably. Only slight changes due to the less OM mineralization such as decrease in PO_4 and NH_3 fluxes and increase in NO_3 intake.

Table 3.1: Mineralization Rates and Flux Estimates for Sulfidic Conditions

BW O_2 (μM)	Oxic Min.	Denit.	MnO_2 Red.	$Fe(OH)_3$ Red.	SO_4 Red.	CH_4	PO_4 flux	NH_3 flux	NO_3 flux	H_2S flux	Mn^{2+} flux	Mn^{3+} flux	Fe^{2+} flux
295	77.1%	14.3%	0.2%	0.3%	8.0%	0.2%	-4.68	-17.25	-22.67	-0.001	0.000	0.000	0.000
140	71.2%	15.6%	0.3%	0.6%	12.0%	0.3%	-4.41	-55.9	17.73	-0.003	0.000	0.000	0.000
80	62.7%	20.8%	0.4%	0.8%	15.0%	0.4%	-4.26	-73.74	44.18	-0.094	0.000	0.000	0.000
40	49.5%	30.9%	0.5%	0.9%	17.8%	0.4%	-4.17	-79.53	63.98	-8.556	0.000	0.000	0.000
5	22.0%	55.2%	0.5%	0.9%	20.9%	0.5%	-4.1	-80.44	90.36	-124.24	-0.025	-0.069	0.000

Table 3.3: Mineralization Rates and Flux Estimates for Suboxic Conditions

BW O_2 (μM)	Oxic Min.	Denit.	MnO_2 Red.	$Fe(OH)_3$ Red.	SO_4 Red.	CH_4	PO_4 flux	NH_3 flux	NO_3 flux	H_2S flux	Mn^{2+} flux	Mn^{3+} flux	Fe^{2+} flux
295	89.26%	10.29%	0.15%	0.29%	0.00%	0.00%	-4.65	-16.94	-24.2	0.000	0.000	0.000	0.000
140	89.51%	9.62%	0.31%	0.56%	0.00%	0.00%	-4.09	-44.5	-11.96	0.000	0.000	0.000	0.000
80	87.19%	11.57%	0.45%	0.79%	0.00%	0.00%	-3.63	-56.28	37.7	0.000	0.000	0.000	0.000
40	80.19%	18.17%	0.60%	1.04%	0.00%	0.00%	-3.11	-55.67	62.85	0.000	0.000	0.000	0.000
5	39.08%	58.64%	0.80%	1.48%	0.00%	0.00%	-2.26	-42.06	127.71	0.000	-0.028	-0.081	0.000

In terms of flux estimations, it is important to consider N:P ratio since nutrients that are entering to the water column are supposed to take place in primary production. In Figures 3.7, 3.8 and 3.9, we see that N:P ratio is mostly controlled by the total N exchange rather than the slight changes in P fluxes. Additionally, in Figure 3.10, we present N:P ratios among changing O_2 levels and under different conditions. It is seen that, under mildly sulfidic and suboxic conditions, decrease of O_2 decreases N:P ratio more than the N:P ratio under sulfidic conditions. Additionally, from this graph, we understand that the benthic flux is richer in terms of phosphorus rather than nitrogen. In accordance with the [65], N:P ratio that we get from fluxes show that it is lower than the OM stoichiometry and dominated by denitrification. Under scarcity of O_2 and SO_4, the less ammonia output and high nitrate input as seen in Tables 3.1,

3.2 and 3.3 leads to this conclusion.

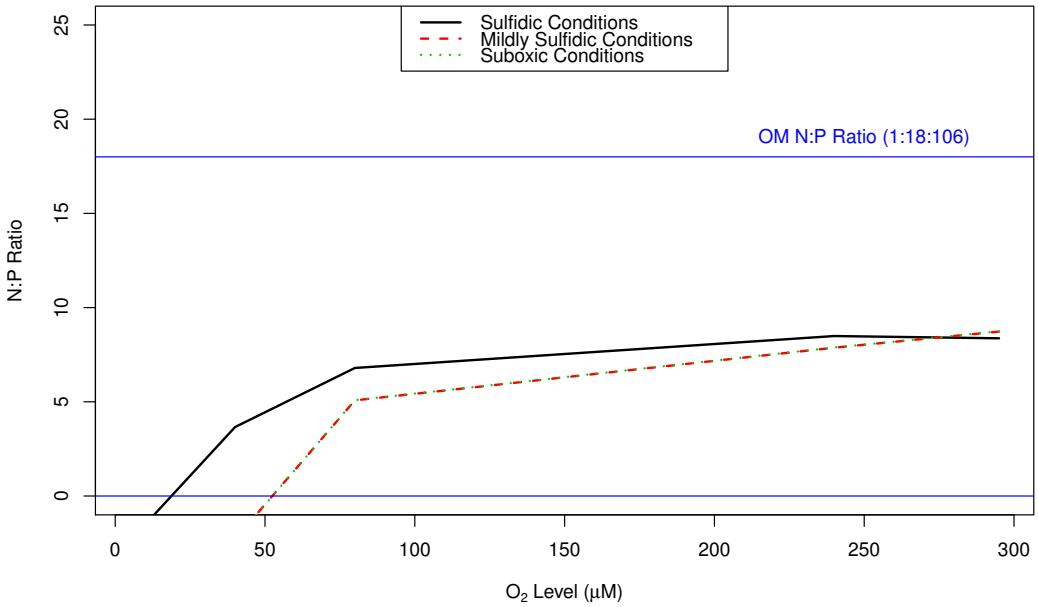

Figure 3.10: N:P Ratio Comparison Among Different Conditions

3.3.3 A Closer Look at P-cycling Under Hypoxia

Since P is a crucial nutrient for marine life that can be supplied from the sediment to the water column and has a potential to promote OAEs [66], in this part we focus on P particularly. In previous experiments PO_4 fluxes are mostly dependent upon OM degradation therefore, this part is dedicated to investigate adsorbed PO_4 and PO_4 coming from OM. Adsorbed PO_4 release due to $Fe(OH)_3$ reduction as a percentage of the total PO_4 release in the sediment can be seen in the Table 3.4. In this table, we see that with decreasing O_2 concentrations, adsorbed PO_4 increases which is due to the decrease in the total OM mineralization. When mildly sulfidic and suboxic conditions are compared, we see that suboxic conditions tend to have higher percentage of PO_4 which can be due to the decrease in OM mineralization and increase in $Fe(OH)_3$ reduction ratio. However, under sulfidic conditions, we expected to have

lower percentages but, it has considerably higher values compared to the other scenarios. This can be explained by the total increase in OM mineralization and also $Fe(OH)_3$ production due to the availability of oxidation pathways such as SO_4 reduction and methanogenesis.

Table 3.4: Adsorbed Phosphate as a percent of Total PO_4 Release

BW O_2 (μM)	Sulfidic	Mildly Suboxic	Suboxic
295	16.16%	2.97%	3.42%
140	16.35%	3.91%	5.12%
80	16.38%	4.40%	6.44%
40	16.39%	4.72%	7.83%
5	16.38%	4.88%	9.72%

3.3.4 Upscaling Flux Estimates

In this part, we aim to demonstrate the importance of benthic fluxes compared to the other nutrients sources such as land runoff and atmospheric deposition. Apart from previous flux estimates which used narrower intervals (1cm) in calculating fluxes, in this part, fluxes are calculated with wider range values (10cm) using Fick's First Law. Resulting values can be seen in Table 3.5 under all three conditions.

The fluxes calculated for the top 1 cm and top 10 cm have been compared with the literature, especially the most recent hypoxic Baltic Sea benthic fluxes as reported by [67]. The 10-cm fluxes compare much better as the very sharp features in phosphate and ammonium gradients within the top 1 cm results in an overestimation of fluxes. In this section, the fluxes have been computed taking Marmara Sea as an example basin for budget comparison. Recently, METU-IMS-lead MARMOD project produced revised estimates of N and P fluxes for the rapidly deoxygenating Marmara Sea, where the stricter management of excessive N and P loads are now considered

Table 3.5: Flux Estimates (μmol cm^{-2}day^{-1}) Using 10cm Sediment Depth

BW O_2 (μM)	PO4 flux	NH3 flux	NO3 flux	H2S flux	MnII flux	MnIII flux	FeII flux
	Sulfidic						
295	-0.19698	-1.11478	-0.16847	-6.38E-05	-8.92E-09	-8.94E-09	-1.77E-08
140	-0.17762	-2.80301	1.727119	-1.60589	-0.00834	-0.00626	-0.07139
80	-0.17261	-3.11352	2.095155	-4.01863	-0.07398	-0.00911	-0.37492
40	-0.1718	-3.16208	2.177513	-5.93117	-0.11891	-0.00811	-0.58863
5	-0.17311	-3.17304	2.197617	-7.67404	-0.15406	-0.00689	-0.77736
	Mildly Sulfidic						
295	-0.18121	-0.70818	-0.40694	-1.26E-08	-7.85E-09	-7.87E-09	-1.30E-08
140	-0.13255	-1.64595	1.342206	-0.00129	-1.53E-06	-1.66E-06	-1.24E-05
80	-0.09669	-1.57289	2.042836	-0.02363	-0.01261	-0.01092	-0.11224
40	-0.0696	-1.15456	2.240958	-0.06319	-0.12521	-0.01818	-0.64292
5	-0.04649	-0.64098	2.234253	-0.12909	-0.22077	-0.01359	-1.25502
	Suboxic						
295	-0.18116	-0.70645	-0.40997	-1.11E-27	-7.84E-09	-7.86E-09	-1.30E-08
140	-0.13231	-1.63824	1.336027	2.18E-29	-1.48E-06	-1.59E-06	-1.07E-05
80	-0.09611	-1.56076	2.038229	-1.04E-31	-0.01145	-0.01039	-0.10544
40	-0.06843	-1.13242	2.240662	-1.68E-31	-0.12395	-0.01838	-0.63731
5	-0.04433	-0.59853	2.234125	0	-0.22111	-0.01371	-1.26027

by the Ministry of Environment.

However, as can be seen in Figure 3.11, benthic fluxes are totally ignored for P and only denitrification was considered for N. Here, using the top 10 cm flux estimates that arise from this thesis, and making the following assumptions we carry on first estimates of benthic fluxes of Marmara Sea:

- Under oxygenated conditions the benthic N and P fluxes may be rapidly oxidized or adsorbed to iron-oxide particles, hence the benthic fluxes will be important for the basin under the hypoxic-anoxic bottom waters of Marmara
- Of the 11,500 km^{-2} of the surface area of the Marmara Sea, it is assumed that 10 percent of this area, 1,150 km^{-2} of seafloor area is currently under the influence of hypoxia or anoxia
- The mildy sulfidic sedimentary biogeochemical conditions will represent the

organic-rich seafloor environment of Marmara, therefore fluxes for this intermediate scenario can be used

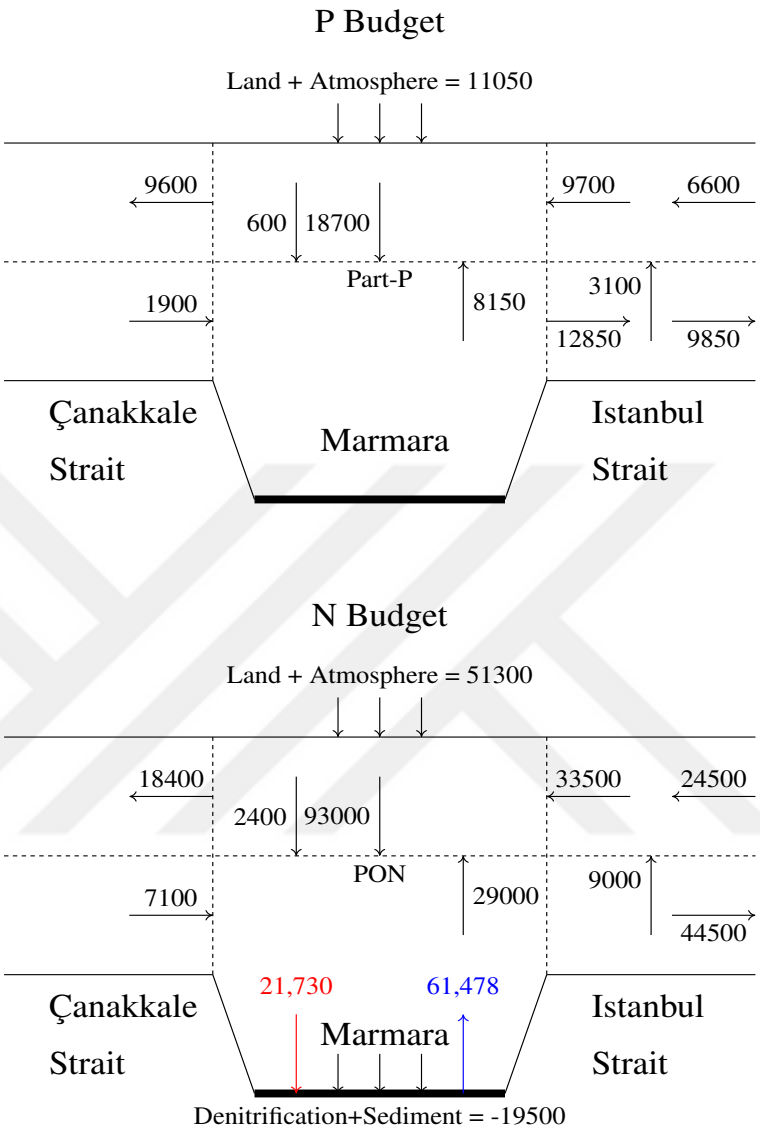

Figure 3.11: Revised N and P Basin-wide Fluxes [68] (tonnes year^{-1}) as a Result of MARMOD Project, Funded by the Ministry of Environment

As a result an average hypoxic PO_4-P flux of 0.07 μmol cm^{-2}d^{-1} and NH_3-N flux of 1.14 μmol cm^{-2}d^{-1} were used. Using the areal estimation above, the resulting basin wide benthic flux for P becomes 9,100 tonnes year^{-1} and for NH_3-N flux it becomes 66,992 tonnes year^{-1}. These are fluxes from the hypoxic seafloor to the bot-

tom waters. For N, there is also an opposing flux which is the denitrification-induced N drawdawn into the sediment. This counter flux (NO_3 intake) is estimated as 1.49 μmol $cm^{-2}d^{-1}$ and translates to 88,722 tonnes of N intake per year. As a result, the net effect of hypoxia is the intake of 21,730 tonnes of N per year (shown with red arrow in Figure 3.11). This independent calculation is very close to the MARMOD estimation of 19,500 tonnes of particulate organic N raining to Marmara Basin .

Additionally, if sulfidic conditions are taken, average NH_3-N flux would be 2.67 μmol $cm^{-2}d^{-1}$ which would add up to 157,095 tonnes per year. Under these conditions, NO_3 intake would be 1.6 μmol $cm^{-2}d^{-1}$ which would be 95,617 tonnes per year in total. Eventually, sediment would release 61,478 tonnes N per year (shown with blue arrow in Figure 3.11). While our results should be taken with caution, as conditions becomes more sulfidic, an interesting conclusion can be that the organic matter remineralization and denitrification in the sediments results in an almost complete benthic turnover of nitrogen in the Marmara Sea, preventing any burial and resulting in the trapping of excess N in the basin waters.

When compared with the combined land and precipitation-based N and P inputs, it can be proposed that the benthic P release estimate (9,100 tonnes $year^{-1}$) is close to the sum of land and precipitation-based inputs (11,050 tonnes $year^{-1}$) and the benthic N release estimate under sulfidic scenario (61,478 tonnes $year^{-1}$) is close to the corresponding inputs (51,100 tonnes $year^{-1}$). Although there are many uncertainties within these estimates, this thesis' results provided the first estimates for the benthic N and P fluxes under hypoxia and demonstrated that the hypoxia-driven nutrient release could be quantitatively as important as land and precipitation-based inputs.

3.3.5 Final Remarks on Modeling Approaches

Similar to the model that is used in this study, most of the models in the literature are tailored to meet the requirements of a certain research study. [33] presents 83

sediment diagenesis modeling studies since 1996. These studies differ in terms of biogeochemistry, transport, solution methodology, modeling approach or additional considerations such as coupling with surrounding environment. These differences are due to the limitations of numerical efficiency because modern day computational power does have constraints. Meaning that, one can not create a model that answers all of the questions about the extremely complex Earth System. It should have some boundary conditions and assumptions to reduce numerical complexity to be able to simulate a focused research topic.

In this model, focus is on the simple analysis of sediment biogeochemistry including anoxic pathways and metal cycles as an adaptation of OMEXDIA model. Therefore, it is a 1D model that is uncoupled from surrounding environment. pH was also out of scope in expense of including broader transport and flux-oriented biogeochemistry. In the following chapter, some future directions to tackle these deficiencies are proposed.

CHAPTER 4

CONCLUSION

Global biogeochemistry is highly dependent on the oceans. There are unique services that oceans do to sustain biogeochemical cycles of the Earth. However, human impacts in form of emissions and waste disposals started to degrade these mechanisms. This trend pose a risk of losing habitability of the Earth either partially or completely. Three main problems of marine environment which are warming, deoxygenation and acidification are known to be irreversible in human time scale [6]. Therefore, it is important to take action before it is too late. To fight with these undesirable outcomes, there are several precautions are made which aim to limit anthropogenic effects on the oceans. Convention on Biodiversity (CBD), regulations of International Seabed Authority (ISA) and Goal 14 of Sustainable Development Goals set by the United Nations are the long-term measures that are taken to reduce potential risk of losing marine ecosystems.

In this study, we focus on sediment biogeochemistry under anoxia/hypoxia and take the Black Sea and Marmara as model systems since the 1D model developed in this thesis will be eventually a sub-module of a larger scale, 3D coupled biogeochemical-physical model of the Marmara and Black Seas. The aim of the thesis is to set up a fundamentally correct, tunable and modular model to provide depth profiles and flux estimates to demonstrate variability under changing oxygen levels. Eventually, we address some future impacts regarding the deoxygenation of the water column due to the benthic input.

In performing this experiments, we used early diagenetic modeling and created a 1D reactive transport model for the sediments which is running on R with the ReacTran package produced by [51]. Model includes 19 species with a full redox cycle, secondary redox reactions, mineral formation and adsorption of phosphate.

In our experiments we consider three alternative scenarios: sulfidic, mildly sulfidic and suboxic. Under these scenarios we take oxygen levels as: 295, 140, 80, 40 and 5 μM. Parameters of the model are obtained from the literature and validation of our model is done by comparing our results with data presented in [60].

Results of our simulations show that, in all scenarios, decrease in oxygen slows down the reoxydation processes which leads to rapid consumption of oxidants after depletion of oxygen. This behavior of the system increases production of metal ions and therefore, corresponding mineral formations.

When conditions move from sulfidic to suboxic, with the decrease in sulfate reduction and methanogenesis, we observe increases in denitrification and reduction of metal oxides. Under these conditions, hydrogen sulfide production greatly decreases which leads to decrease in sulfide based mineral formation.

Flux estimates show that, under sulfidic conditions there is a substantial amount of hydrogen sulfide input to the water column which decreases when conditions become suboxic. Under mildly sulfidic and suboxic conditions we observe less ammonia and phosphate fluxes to the water column due to less OM mineralization. Due to the scarcity of sulfate reduction, denitrification becomes more important than sulfidic conditions and sediments takes up more nitrate from the water column. Additionally, metal fluxes exists when oxygen is at critical levels and increases further when conditions are suboxic.

Another analysis on N:P ratios show that, when sediment becomes anoxic, N:P ratio decreases under all scenarios due to lower OM mineralization. However, since mildly sulfidic and suboxic conditions have more nitrate intake instead of ammonia release, N:P ratios decrease even further compared to the sulfidic conditions. Analysis on N:P ratios also show that, estimated N:P ratios are under OM stoichiometry that is used in the simulations.

Results on investigation of phosphate show that, adsorbed phosphate takes small percentages of total phosphate release which slightly increases with the decreasing oxygen due to the decrease in OM mineralization.

Upscaling our flux estimates and comparison with calculations derived from the METU-IMS lead MARMOD Project showed that in the Marmara Sea, an estimated phosphate flux to the water column exists. Additionally, the sediment of the Marmara is a sink for N under mildly sulfidic conditions and becomes a source when conditions changes to sulfidic.

One important conclusion that we get from this study is the importance of OM rain rate. Since most of our results are very sensitive to OM mineralization, we can say that along with many uncertainties included in the model, OM rain rate should be correctly measured to successfully create biogeochemical profiles and flux estimates using this type of modeling study.

In summary, it is a modeling work aimed to create a basic and useful model from a simple existing modeling framework to analyze sediment biogeochemistry under changing oxygen levels. It can be further developed to analyze different conditions by introducing new species, reaction or transport parameters or it can be basically used as a tool to understand feedbacks to the water column.

An important improvement can include modeling of bioturbation. Bioturbation intensity can be considered and bioturbation coefficient can be oxygen-dependent as in [37] to make model more sensitive to changing oxygen levels. One step further would be to take this model into multi dimensional form to understand effects of land input such as point sources in sediment biogeochemistry. Another extension could be a coupling with the water column to simulate biogeochemical dynamics across two environments and even combining it with multi dimensional models such as [49, 50]. While coupling with water column, the Black Sea oceanographic conditions affecting biogeochemistry such as CIL and FPL should be considered. In case of Marmara, coupling would be difficult because of the complex oceanographic conditions with the Bosphorus jet and two straits. Apart from coupling with water column, as in [49] where they include benthic algae in their model, coupling with ecology is also an important approach for future studies. Another approach would focus more on fluxes by including factors such as sediment resuspension [69] to more accurately estimate nutrient and toxin input to the water column. One important extension would be including pH because deoxygenation and ocean acidification are known to have synergistic effects in marine environment [70]. Another different approach can be to take this modeling framework into a more long-term processes oriented form. By doing this, paleoenvironmental conditions can be analyzed using deep burial processes and transport of stable isotopes with proper parametrization. However, to study long-term processes one should consider long-term oscillations such as oxygen concentrations.

REFERENCES

[1] L. R. Kump, J. F. Kasting, and R. G. Crane, *The Earth System*. San Francisco, CA: Prentice Hall, 2010.

[2] R. K. Pachauri and A. Reisinger, "Ipcc fourth assessment report," in *Climate change 2007: impacts, adaptation and vulnerability*, Geneva: IPCC, 2007.

[3] J. T. Houghton, Y. D. J. G. Ding, D. J. Griggs, M. Noguer, P. J. van der Linden, X. Dai, and C. A. Johnson, *Climate change 2001: the scientific basis*. The Press Syndicate of the University of Cambridge, 2001.

[4] J. Hansen, M. Sato, R. Ruedy, K. Lo, D. W. Lea, and M. Medina-Elizade, "Global temperature change," *Proceedings of the National Academy of Sciences*, vol. 103, no. 39, pp. 14288–14293, 2006.

[5] T. R. Karl and K. E. Trenberth, "Modern global climate change," *Science*, vol. 302, pp. 1719–1723, 2003.

[6] N. Gruber, "Warming up, turning sour, losing breath: ocean biogeochemistry under global change," *Phil. Trans. R. Soc. A*, vol. 369, p. 1980–1996, 2011.

[7] O. Hoegh-Guldberg and J. F. Bruno, "The impact of climate change on the world's marine ecosystems," *Science*, vol. 328, pp. 1523–1528, 2010.

[8] C. L. Sabine, R. A. Feely1, N. Gruber, R. M. Key, K. Lee, J. L. Bullister, R. Wanninkhof, C. S. Wong, D. W. R. Wallace, B. Tilbrook, F. J. Millero, T.-H. Peng, A. Kozyr, T. Ono, and A. F. Rios, "The oceanic sink for anthropogenic CO_2," *Science*, vol. 305, pp. 367–371, 2004.

[9] N. R. Bates, S. B. Moran, D. A. Hansell, and J. T. Mathis, "An increasing CO_2 sink in the arctic ocean due to sea ice loss," *Geophysical Research Letters*, vol. 33, 2006.

[10] S. Libes, *Introduction to marine biogeochemistry*. Academic Press, 2011.

[11] N. Gruber, "The marine nitrogen cycle: overview and challenges," in *Nitrogen in the marine environment* (M. R. M. Douglas G Capone, Deborah A Bronk and E. J. Carpenter, eds.), ch. 1, pp. 1–50, Elsevier, 2008.

[12] M. Dumitrescu and S. C. Brassell, "Biogeochemical assessment of sources of organic matter and paleoproductivity during the early aptian oceanic anoxic event at shatsky rise, odp leg 198," *Organic Geochemistry*, vol. 36, no. 7, pp. 1002–1022, 2005.

[13] A. H. Altieri and K. B. Gedan, "Climate change and dead zones," *Global Change Biology*, vol. 21, pp. 1395–1406, 2014.

[14] R. F. Keeling, A. Körtzinger, , and N. Gruber, "Ocean deoxygenation in a warming world," *Annual Review of Marine Science*, vol. 2, pp. 199–229, 2010.

[15] D. Archer, P. Martin, B. Buffett, V. Brovkin, S. Rahmstorf, and A. Ganopolski, "The importance of ocean temperature to global biogeochemistry," *Earth and Planetary Science Letters*, vol. 222, no. 2, pp. 333–348, 2004.

[16] N. N. Rabalais, R. J. Diaz, L. A. Levin, R. E. Turner, D. Gilbert, and J. Zhang, "Dynamics and distribution of natural and human-caused hypoxia," *Biogeosciences*, vol. 7, no. 2, p. 585, 2010.

[17] R. J. Diaz and R. Rosenberg, "Spreading dead zones and consequences for marine ecosystems," *Science*, vol. 321, pp. 926–929, 2008.

[18] A. Bakun and S. J. Weeks, "Greenhouse gas buildup, sardines, submarine eruptions and the possibility of abrupt degradation of intense marine upwelling ecosystems," *Ecology Letters*, vol. 7, no. 11, pp. 1015–1023, 2004.

[19] L. R. Kump, A. Pavlov, and M. A. Arthur, "Massive release of hydrogen sulfide to the surface ocean and atmosphere during intervals of oceanic anoxia," *Geology*, vol. 33, no. 5, pp. 397–400, 2005.

[20] F. Chan, J. A. Barth, J. Lubchenco, A. Kirincich, H. Weeks, W. T. Peterson,

and B. A. Menge, “Emergence of anoxia in the california current large marine ecosystem,” *Science*, vol. 319, no. 5865, pp. 920–920, 2008.

[21] R. Vaquer-Sunyer and C. M. Duarte, “Thresholds of hypoxia for marine biodiversity,” *Proceedings of the National Academy of Sciences*, vol. 105, no. 40, pp. 15452–15457, 2008.

[22] R. A. Feely, S. R. Alin, J. Newton, C. L. Sabine, M. Warner, A. Devol, C. Krembs, and C. Maloy, “The combined effects of ocean acidification, mixing, and respiration on ph and carbonate saturation in an urbanized estuary,” *Estuarine, Coastal and Shelf Science*, vol. 88, no. 4, pp. 442–449, 2010.

[23] B. P. Boudreau, “The mathematics of early diagenesis: from worms to waves,” *Reviews of Geophysics*, vol. 38, no. 3, pp. 389–416, 2000.

[24] K. Stewart, S. Kassakian, M. Krynytzky, D. DiJulio, and J. W. Murray, “Oxic, suboxic, and anoxic conditions in the black sea,” in *The Black Sea flood question: Changes in coastline, climate, and human settlement*, pp. 1–21, Springer, 2007.

[25] E. Yakushev, V. Chasovnikov, J. Murray, S. Pakhomova, O. Podymov, and P. Stunzhas, “Vertical hydrochemical structure of the black sea,” in *The Black Sea Environment*, pp. 277–307, Springer, 2007.

[26] R. Gerin, P.-M. Poulain, Ş. T. Beşiktepe, and P. Zanasca, “On the surface circulation of the marmara sea as deduced from drifters,” *Turkish Journal of Earth Sciences*, vol. 22, no. 6, pp. 919–930, 2013.

[27] R. A. Berner, *Early Diagenesis: A Theoretical Approach*. Princeton University Press, 1980.

[28] B. P. Boudreau, *Diagenetic Models and Their Implementation*. New York, NY: Springer, 1997.

[29] P. Van Cappellen, J.-F. Gaillard, and C. Rabouille, “Biogeochemical transformations in sediments: kinetic models of early diagenesis,” in *Interactions of C, N, P and S biogeochemical cycles and global change*, pp. 401–445, Springer, 1993.

[30] K. Soetaert, P. M. J. Herman, and J. J. Middelburg, "A model of early diagenetic processes from the shelf to abyssal depths," *Geochimica et Cosmochimica Acta*, vol. 60, pp. 1019–1040, 1996.

[31] P. V. Capellen and Y. Wang, "Cycling of iron and manganese in surface sediments: a general theory for the coupled transport and reaction of carbon, oxygen, nitrogen, sulfur, iron, and manganese," *American Journal of Science*, vol. 296, pp. 197–243, 1996.

[32] A. W. Dale, S. Sommer, L. Bohlen, T. Treude, V. J. Bertics, H. W. Bange, O. Pfannkuche, T. Schorp, M. Mattsdotter, and K. Wallmann, "Rates and regulation of nitrogen cycling in seasonally hypoxic sediments during winter (boknis eck, sw baltic sea): Sensitivity to environmental variables," *Estuarine, Coastal and Shelf Science*, vol. 95, no. 1, pp. 14–28, 2011.

[33] D. W. Paraska, M. R. Hipsey, and S. U. Salmon, "Sediment diagenesis models: Review of approaches, challenges and opportunities," *Environmental Modelling & Software*, vol. 61, pp. 297–325, 2014.

[34] R. Richter, "Fluidal-textur in sediment-gesteinen und ber sedifluktion berhaupt," *Notizbl Hess L-Amt Bodenforsch*, vol. 6, pp. 67–81, 1952.

[35] B. P. Boudreau, "The diffusive tortuosity of fine-grained unlithified sediments," *Geochimica et Cosmochimical Acta*, vol. 60, pp. 3139–3142, 1996.

[36] H. Fossing, P. Berg, B. Thamdrup, S. Rysgaard, H. Sorensen, and K. Nielsen, "A model set-up for an oxygen and nutrient flux model for aarhus bay (denmark)," *NERI technical report*, vol. 483, 2004.

[37] K. Soetaert and J. J. Middelburg, "Modeling eutrophication and oligotrophication of shallow-water marine systems: the importance of sediments under stratified and well-mixed conditions," *Hydrobiologia*, vol. 629, no. 1, pp. 239–254, 2009.

[38] D. C. Reed, C. P. Slomp, and G. J. de Lange, "A quantitative reconstruction of organic matter and nutrient diagenesis in mediterranean sea sediments over the

holocene," *Geochimica et Cosmochimica Acta*, vol. 75, no. 19, pp. 5540–5558, 2011.

[39] C. Meile, C. M. Koretsky, and P. V. Cappellen, "Quantifying bioirrigation in aquatic sediments: an inverse modeling approach," *Limnology and oceanography*, vol. 46, no. 1, pp. 164–177, 2001.

[40] K. Stolpovsky, A. W. Dale, and K. Wallmann, "A new look at the multi-g model for organic carbon degradation in surface marine sediments for coupled benthic-pelagic simulations of the global ocean," *Biogeosciences Discussions*, 2017.

[41] J. J. Middelburg, "A simple rate model for organic matter decomposition in marine sediments," *Geochimica et Cosmochimica Acta*, vol. 53, no. 7, pp. 1577–1581, 1989.

[42] P. Froelich, G. Klinkhammer, and M. Bender, "Early oxidation of organic matter in pelagic sediments of the eastern equatorial atlantic: suboxic diagenesis," *Geochimica et Cosmochimica Actaet Cosmochimica Acta*, vol. 43, pp. 1075–1090, 1979.

[43] S. Arndt, B. B. Jørgensen, D. E. LaRowe, J. Middelburg, R. Pancost, and P. Regnier, "Quantifying the degradation of organic matter in marine sediments: a review and synthesis," *Earth-science reviews*, vol. 123, pp. 53–86, 2013.

[44] B. P. Boudreau and J. T. Westrich, "The dependence of bacterial sulfate reduction on sulfate concentration in marine sediments," *Geochimica et cosmochimica acta*, vol. 48, no. 12, pp. 2503–2516, 1984.

[45] S. P. Dhakar and D. J. Burdige, "A coupled, non-linear, steady state model for early diagenetic processes in pelagic sediments," *American Journal of Science*, vol. 296, no. 3, 1996.

[46] A. S. Madison, *Biogeochemical Cycling of Soluble Manganese(III) in Marine (Pore)Waters*. PhD thesis, University of Delaware, 2012.

[47] D. C. Reed, C. P. Slomp, and B. G. Gustafsson, "Sedimentary phosphorus dynamics and the evolution of bottom-water hypoxia: A coupled benthic-pelagic

model of a coastal system," *Limnology and Oceanography*, vol. 56, no. 3, pp. 1075–1092, 2011.

[48] I. Tsandev, D. C. Reed, and C. P. Slomp, "Phosphorus diagenesis in deep-sea sediments: Sensitivity to water column conditions and global scale implications," *Chemical Geology*, vol. 330, pp. 127–139, 2012.

[49] A. Sohma, Y. Sekiguchi, and K. Nakata, "Modeling and evaluating the ecosystem of sea-grass beds, shallow waters without sea-grass, and an oxygen-depleted offshore area," *Journal of marine systems*, vol. 45, no. 3-4, pp. 105–142, 2004.

[50] A. Sohma, Y. Sekiguchi, T. Kuwae, and Y. Nakamura, "A benthic–pelagic coupled ecosystem model to estimate the hypoxic estuary including tidal flat—model description and validation of seasonal/daily dynamics," *Ecological modelling*, vol. 215, no. 1-3, pp. 10–39, 2008.

[51] K. Soetaert and F. Meysman, "R-package reactran: Reactive transport modelling in r," *Environmental Modelling & Software*, vol. 32, pp. 49–60, 2012.

[52] G. W. Luther, "Manganese(ii) oxidation and mn(iv) reduction in the environment—two one-electron transfer steps versus a single two electron step," *Geomicrobiology Journal*, vol. 22, pp. 195–203, 2005.

[53] W. v. Engelhardt, *The origin of sediments and sedimentary rocks*. Schweizerbart'sche Verlagsbuchhandlung, 1977.

[54] J. Crank, *The Mathematics of Diffusion*. Oxford Science Publications, 1975.

[55] J. W. M. Wijsman, P. M. J. Herman, J. J. Middelburg, and K. Soetaert, "A model for early diagenetic processes in sediments of the continental shelf of the black sea," *Estuarine, Coastal and Shelf Science*, vol. 54, pp. 403–421, 2002.

[56] A. W. Dale, V. J. Bertics, T. Treude, S. Sommer, and K. Wallmann, "Modeling benthic–pelagic nutrient exchange processes and porewater distributions in a seasonally hypoxic sediment: evidence for massive phosphate release by beggiatoa?," *Biogeosciences*, vol. 10, no. 2, pp. 629–651, 2013.

[57] A. C. Hindmarsh, "Lsode and lsodi, two new initial value ordinary differential equation solvers," *ACM Signum Newsletter*, vol. 15, no. 4, pp. 10–11, 1980.

[58] K. Soetaert, T. Petzoldt, and R. W. Setzer, "Solving differential equations in r: package desolve," *Journal of Statistical Software*, vol. 33, 2010.

[59] G. W. Luther III, T. M. Church, and D. Powell, "Sulfur speciation and sulfide oxidation in the water column of the black sea," *Deep Sea Research Part A. Oceanographic Research Papers*, vol. 38, pp. S1121–S1137, 1991.

[60] M. Yücel, S. K. Konovalov, T. S. Moore, C. P. Janzen, and G. W. Luther III, "Sulfur speciation in the upper black sea sediments," *Chemical Geology*, vol. 269, no. 3-4, pp. 364–375, 2010.

[61] T. Oguz, J. W. Murray, and A. E. Callahan, "Modeling redox cycling across the suboxic–anoxic interface zone in the black sea," *Deep Sea Research Part I: Oceanographic Research Papers*, vol. 48, no. 3, pp. 761–787, 2001.

[62] W. Ludwig, E. Dumont, M. Meybeck, and S. Heussner, "River discharges of water and nutrients to the mediterranean and black sea: major drivers for ecosystem changes during past and future decades?," *Progress in Oceanography*, vol. 80, no. 3, pp. 199–217, 2009.

[63] O. Yiğiterhan and J. W. Murray, "Trace metal composition of particulate matter of the danube river and turkish rivers draining into the black sea," *Marine Chemistry*, vol. 111, no. 1-2, pp. 63–76, 2008.

[64] S. Medinets and V. Medinets, "Investigations of atmospheric wet and dry nutrient deposition to marine surface in western part of the black sea," 2012.

[65] S. Tugrul, O. Basturk, C. Saydam, and A. Yilmaz, "Changes in the hydrochemistry of the black sea inferred from water density profiles," *Nature*, vol. 359, no. 6391, p. 137, 1992.

[66] A. J. Watson, T. M. Lenton, and B. J. Mills, "Ocean deoxygenation, the global phosphorus cycle and the possibility of human-caused large-scale ocean anoxia," *Phil. Trans. R. Soc. A*, vol. 375, no. 2102, p. 20160318, 2017.

[67] S. Sommer, D. Clemens, M. Yücel, O. Pfannkuche, P. O. Hall, E. Almroth-Rosell, H. N. Schulz-Vogt, and A. W. Dale, "Major bottom water ventilation events do not significantly reduce basin-wide benthic n and p release in the eastern gotland basin (baltic sea)," *Frontiers in Marine Science*, vol. 4, p. 18, 2017.

[68] C. Polat and S. Tugrul, "Chemical exchange between the mediterranean and the black sea via the turkish straits," *Bulletin de l'Institut océanographique*, pp. 167–186, 1996.

[69] A. Massoudieh, F. A. Bombardelli, and T. R. Ginn, "A biogeochemical model of contaminant fate and transport in river waters and sediments," *Journal of contaminant hydrology*, vol. 112, no. 1-4, pp. 103–117, 2010.

[70] A. Oschlies, K. G. Schulz, U. Riebesell, and A. Schmittner, "Simulated 21st century's increase in oceanic suboxia by co2-enhanced biotic carbon export," *Global Biogeochemical Cycles*, vol. 22, no. 4, 2008.

APPENDIX A

MODEL PARAMETERS

Table A.1: Model Parameters

	[46]		[55]		[48]		[47]	
Parameter	**Value**	**Units**	**Value**	**Units**	**Value**	**Units**	**Value**	**Units**
OM1 flux	30	μmol cm^{-2} yr^{-1}	N/A	-	7.5	μmol cm^{-2} yr^{-1}	N/A	-
OM2 flux	210	μmol cm^{-2} yr^{-1}	N/A	-	7.5	μmol cm^{-2} yr^{-1}	N/A	-
Sediment Density	2.65	g cm^{-3}	N/A	-	N/A	-	2.65	g cm^{-3}
OM1/(OM1+OM2)	0.125	-	0.29	-	0.9	-	N/A	-
BW O2	60	μmol L^{-1}	295	μM	180	μM	N/A	-
BW NO3	25	μmol L^{-1}	5	μM	30	μM	N/A	-
BW MnO2(flux)	0.9	μmol cm^{-2} yr^{-1}	0.01	μmol cm^{-2} day^{-1}	0.02	μmol cm^{-2} day^{-1}	0.003	μmol cm^{-2} yr^{-1}
BW FeOH3(flux)	5	μmol cm^{-2} yr^{-1}	0.028	μmol cm^{-2} day^{-1}	0.1	μmol cm^{-2} day^{-1}	5.75	μmol cm^{-2} yr^{-1}
BW SO4	2.87E+04	μmol L^{-1}	1.60E+04	μM	2.80E+04	μM	1.20E+04	μM
BW PO4	4	μmol L^{-1}	N/A	-	N/A	-	N/A	-
BW NH4	0	μmol L^{-1}	0.58	μM	0	μM	0.18	μM
BW H2S	0	μmol L^{-1}	0	μM	N/A	-	N/A	-
BW MnII	0	μmol L^{-1}	0	μM	0	μM	N/A	-
BW MnIII	0	μmol L^{-1}	N/A	-	N/A	-	N/A	-
BW FeII	0	μmol L^{-1}	0	μM	0	μM	N/A	-
BW CO2	2.44	μmol L^{-1}	N/A	-	N/A	-	N/A	-
BW CH4	0	μmol L^{-1}	0	μM	N/A	-	N/A	-
FeS flux	0	μmol cm^{-2} yr^{-1}	0	μmol cm^{-2} day^{-1}	N/A	-	N/A	-
S0 flux	0	μmol cm^{-2} yr^{-1}	N/A		N/A	-	N/A	-
FeS2 flux	0	μmol cm^{-2} yr^{-1}	0	μmol cm^{-2} day^{-1}	N/A	-	N/A	-
MnCO3 flux	0	μmol cm^{-2} yr^{-1}	N/A		N/A	-	N/A	-
FeCO3 flux	0	μmol cm^{-2} yr^{-1}	N/A		N/A	-	N/A	-
Porosity at the SWI	0.9	-	0.95	-	N/A	-	0.943	-
Porosity at infinite depth	0.79	-	0.73	-	N/A	-	0.877	-
Porosity at.coef.	0.25	-	0.23	-	N/A	-	N/A	-
Burial velocity	0.2	cm yr^{-1}	0.0003	cm day^{-1}	0.001	cm yr^{-1}	N/A	-
Bioturbation at the SWI	5	cm^2 yr^{-1}	0.033	cm^2 day^{-1}	0.24 (0 for anoxic)	cm^2 yr^{-1}	N/A	-
Bioturbation half-mixing depth	10	cm	1	cm	5 (0 for anoxic)	cm	N/A	-

Table A.1: Continued

	[46]		[55]		[48]		[47]	
Parameter	**Value**	**Units**	**Value**	**Units**	**Value**	**Units**	**Value**	**Units**
Temperature	5	°C	5.8	°C	2	°C	3.3-13.7	°C
OM stoichiometry	106:18:01	mol:mol:mol	106:16:01	mol:mol:mol	200:21:01	mol:mol:mol	106:16:01	mol:mol:mol
Fe-P ads.rate	N/A	-	N/A	-	0.01	-	0.175	-
Half-sat. O2	1	μmol L^{-1}	3.1	μmol L^{-1}	20	μmol L^{-1}	20	μmol L^{-1}
Half-sat. NO3	4	μmol L^{-1}	30	μmol L^{-1}	4	μmol L^{-1}	4	μmol L^{-1}
Half-sat. MnO2	4	μmol g^{-1}	5000	μmol L^{-1}	4	μmol g^{-1}	4	μmol g^{-1}
Half-sat. FeOH	60	μmol g^{-1}	12500	μmol L^{-1}	65	μmol g^{-1}	65	μmol g^{-1}
Half-sat. SO4	1000	μmol L^{-1}	1620	μmol L^{-1}	1.6	μmol L^{-1}	1.6	μmol L^{-1}
Atten.coef. for SO4 and CH4	7.50E-02	-	N/A	-	7.00E-04	-	7.50E-02	-
OM1 degradation constant	1.3	yr^{-1}	0.0753	day^{-1}	0.15	yr^{-1}	1.62	yr^{-1}
OM2 degradation constant	0.01	yr^{-1}	0.003	day^{-1}	0.0015	yr^{-1}	0.0086	yr^{-1}
Rate constant for nitrification	100	μmol^{-1} L yr^{-1}	20	μmol^{-1} L day^{-1}	10	μmol^{-1} L yr^{-1}	10	μmol^{-1} L yr^{-1}
Rate constant for MnII oxidation	1000	μmol^{-1} L yr^{-1}	0.0137	μmol^{-1} L day^{-1}	20	μmol^{-1} L yr^{-1}	20	μmol^{-1} L yr^{-1}
Rate constant MnIII oxidation	100	μmol^{-1} L yr^{-1}	N/A	-	N/A	-	N/A	-
Rate constant FeII oxidation	35	μmol^{-1} L yr^{-1}	2.94E-01	μmol^{-1} L day^{-1}	140	μmol^{-1} L yr^{-1}	140	μmol^{-1} L yr^{-1}
Rate constant H2S oxidation	16	μmol^{-1} L yr^{-1}	4.38E-04	μmol^{-1} L day^{-1}	0.16	μmol^{-1} L yr^{-1}	0.16	μmol^{-1} L yr^{-1}
Rate constant CH4 oxidation	100	μmol^{-1} L yr^{-1}	2.74E+01	μmol^{-1} L day^{-1}	10000	μmol^{-1} L yr^{-1}	10000	μmol^{-1} L yr^{-1}
Rate constant FeS oxidation	1	μmol^{-1} L yr^{-1}	8.22E-04	μmol^{-1} L day^{-1}	0.3	μmol^{-1} L yr^{-1}	0.3	μmol^{-1} L yr^{-1}
Rate constant FeS2 oxidation	0.02	μmol^{-1} L yr^{-1}	4.38E-04	μmol^{-1} L day^{-1}	0.001	μmol^{-1} L yr^{-1}	0.001	μmol^{-1} L yr^{-1}
Rate constant FeII MnO2 ox.	0.01	μmol^{-1} L yr^{-1}	8.22E-03	μmol^{-1} L day^{-1}	10	μmol^{-1} L yr^{-1}	0.002	μmol^{-1} L yr^{-1}
Rate constant FeII MnIII	1	μmol^{-1} L yr^{-1}	N/A	-	N/A	μmol^{-1} L yr^{-1}		μmol^{-1} L yr^{-1}
Rate constant H2S MnO2 ox.	0.02	μmol^{-1} L yr^{-1}	5.48E-05	μmol^{-1} L day^{-1}	0.02	μmol^{-1} L yr^{-1}	0.02	μmol^{-1} L yr^{-1}
Rate constant H2S MnIII	0	μmol^{-1} L yr^{-1}	N/A	-	N/A	-	N/A	-
Rate constant MnII NO3 ox.	10	μmol^{-1} L yr^{-1}	N/A	-	N/A	-	N/A	-
Rate constant H2S NO3 ox.	10	μmol^{-1} L yr^{-1}	N/A	-	N/A	-	N/A	-
Rate constant S0 ox.	0.1	yr^{-1}	N/A	-	0.003	μmol^{-1} L yr^{-1}	0.003	μmol^{-1} L yr^{-1}
Rate constant H2S FeOH ox.	0.01	μmol^{-1} L yr^{-1}	1.00E-07	μmol^{-1} L day^{-1}	0.008	μmol^{-1} L yr^{-1}	0.008	μmol^{-1} L yr^{-1}
Rate constant FeS H2S	0.2	μmol^{-1} L yr^{-1}	8.90E-06	μmol^{-1} L day^{-1}	N/A	-	N/A	-
Rate constant CH4 SO4 ox.	0.01	μmol^{-1} L yr^{-1}	2.74E-05	μmol^{-1} L day^{-1}	0.01	μmol^{-1} L yr^{-1}	0.01	μmol^{-1} L yr^{-1}
Rate constant FeII H2S	1	μmol^{-1} L yr^{-1}	1	μmol^{-1} L day^{-1}	0.1	μmol^{-1} L yr^{-1}	0.1	μmol^{-1} L yr^{-1}
Rate constant MnII CO3	0.001	μmol^{-1} L yr^{-1}	N/A	-	N/A	-	N/A	-

Table A.1: Continued

	[46]		[55]		[48]		[47]	
Parameter	**Value**	**Units**	**Value**	**Units**	**Value**	**Units**	**Value**	**Units**
Saturation constant MnCO3	1.00E-04	μmol^{-2} L^{-2}	N/A	-	N/A	-	N/A	-
Rate constant MnCO3 diss.	0.25	yr^{-1}	N/A	-	N/A	-	N/A	-
Rate constant FeII CO3	0.01	μmol^{-1} L yr^{-1}	N/A	-	N/A	-	N/A	-
Saturation constant FeCO3	1.00E-04	μmol^{-2} L^{-2}	N/A	-	N/A	-	N/A	-
Rate constant FeCO3 diss.	0.25	yr^{-1}	N/A	-	N/A	-	N/A	-
Adsorption coefficient ammonia	1.4	-	1.3	-	N/A	-	N/A	-
Rate constant FeS diss.	N/A	-	2.74E-06	day^{-1}	N/A	-	N/A	-
Saturation constant FeS	N/A	-	6310	μmol L^{-1}	N/A	-	N/A	-
Half-sat. SO4 methanogen. inhib.	N/A	-	1000	μmol L^{-1}	3.2	μmol L^{-1}	N/A	-
Half-sat. FeOH methanogen. inhib.	N/A	-	12500	μmol L^{-1}	130	μmol L^{-1}	N/A	-
Half-sat. FeOH SO4 red. inhib.	N/A	-	12500	μmol L^{-1}	130	μmol L^{-1}	N/A	-
Half-sat. MnO2 methanogen. inhib.	N/A	-	5000	μmol L^{-1}	8	μmol L^{-1}	N/A	-
Half-sat. MnO2 SO4 red. inhib.	N/A	-	5000	μmol L^{-1}	8	μmol L^{-1}	N/A	-
Half-sat. MnO2 FeOH red. inhib.	N/A	-	5000	μmol L^{-1}	8	μmol L^{-1}	N/A	-
Half-sat. NO3 methanogen .inhib.	N/A	-	10	μmol L^{-1}	8	μmol L^{-1}	N/A	-
Half-sat. NO3 SO4 red. inhib.	N/A	-	10	μmol L^{-1}	8	μmol L^{-1}	N/A	-
Half-sat. NO3 FeOH red. inhib.	N/A	-	10	μmol L^{-1}	8	μmol L^{-1}	N/A	-
Half-sat. NO3 MnO2 red. inhib.	N/A	-	10	μmol L^{-1}	8	μmol L^{-1}	N/A	-
Half-sat. O2 methanogen. inhib.	N/A	-	8	μmol L^{-1}	40	μmol L^{-1}	N/A	-
Half-sat. O2 SO4 red. inhib.	N/A	-	8	μmol L^{-1}	40	μmol L^{-1}	N/A	-
Half-sat. O2 FeOH red. inhib.	N/A	-	8	μmol L^{-1}	40	μmol L^{-1}	N/A	-
Half-sat. O2 MnO2 red. inhib.	N/A	-	8	μmol L^{-1}	40	μmol L^{-1}	N/A	-
Half-sat. O2 denitrif. inhib.	N/A	-	10	μmol L^{-1}	40	μmol L^{-1}	N/A	-

APPENDIX B

SOURCE CODE OF THE SIMULATION MODEL

```
# This computer code is a customized version of OMEXDIA
# (Soetaert et al., 1996) model to be used as a simulation
# tool for the Master's Thesis study of Kadir Bice in Earth
# System Science Program at Middle East Technical University

pHincluded <- 0
OMEXDIA_kb <-function(time = 0,     # time = 0 for steady-state
state,        # species to be modeled
parms,        # parameter values
...)  {

with (as.list(parms), {

FDET  <- state[1:N]
SDET  <- state[(N+1)  :(2*N)]
O2    <- state[(2*N+1):(3*N)]
NO3   <- state[(3*N+1):(4*N)]
NH3   <- state[(4*N+1):(5*N)]
CH4   <- state[(5*N+1):(6*N)]
MnO2  <- state[(6*N+1):(7*N)]
MnII  <- state[(7*N+1):(8*N)]
FeOH  <- state[(8*N+1):(9*N)]
FeII  <- state[(9*N+1):(10*N)]
SO4   <- state[(10*N+1):(11*N)]
H2S   <- state[(11*N+1):(12*N)]
FeS   <- state[(12*N+1):(13*N)]
FeS2  <- state[(13*N+1):(14*N)]
MnIII <- state[(14*N+1):(15*N)]
```

```
S0    <- state[(15*N+1):(16*N)]
FeCO3 <- state[(16*N+1):(17*N)]
MnCO3 <- state[(17*N+1):(18*N)]
CO3   <- state[(18*N+1):(19*N)]
PO4   <- state[(19*N+1):(20*N)]
FeP   <- state[(20*N+1):(21*N)]
if(pHincluded == 1){
H     <- state[(21*N+1):(22*N)]}

# ---------------------------------------
# Transport
# ---------------------------------------

Flux  <- MeanFlux

# Solids
FDETtran <- tran.1D(C = FDET, flux.up = Flux*pFast, D = DbGrid, v = uGrid,
AFDW = 0.5, VF = porGridSolid, dx = Grid)

SDETtran <- tran.1D(C = SDET, flux.up = Flux*(1-pFast), D = DbGrid, v = uGrid,
AFDW = 0.5, VF = porGridSolid, dx = Grid)

MnO2tran <- tran.1D (C = MnO2, C.up = bwMnO2, D = DispMnII, v = uGrid,
AFDW = 0.5,  VF = porGridSolid, dx = Grid)

FeOHtran <- tran.1D (C = FeOH, C.up = bwFeOH, D = DispFeII, v = uGrid,
AFDW = 0.5, VF = porGridSolid, dx = Grid)

FeStran <- tran.1D (C = FeS, flux.up = bwFeS, D = DbGrid, v = uGrid,
AFDW = 0.5, VF = porGridSolid, dx = Grid)

FeS2tran <- tran.1D (C = FeS2, flux.up = bwFeS2, D = DbGrid, v = uGrid,
AFDW = 0.5, VF = porGridSolid, dx = Grid)

S0tran <- tran.1D (C = S0, flux.up = bwS0, D = DbGrid, v = uGrid,
AFDW = 0.5, VF = porGridSolid, dx = Grid)

FeCO3tran <- tran.1D (C = FeCO3, flux.up = bwFeCO3, D = DbGrid, v = uGrid,
AFDW = 0.5, VF = porGridSolid, dx = Grid)
```

```
MnCO3tran <- tran.1D (C = MnCO3, flux.up = bwMnCO3, D = DbGrid, v = uGrid,
AFDW = 0.5, VF = porGridSolid, dx = Grid)

FePtran <- tran.1D (C = FeP, C.up = bwFeP, D = DispFeII, v = uGrid,
AFDW = 0.5, VF = porGridSolid, dx = Grid)

# Solutes
O2tran  <- tran.1D (C = O2, C.up = bwO2, D = DispO2, v = vGrid,
VF = porGrid, dx = Grid)

NO3tran <- tran.1D (C = NO3, C.up = bwNO3, D = DispNO3, v = vGrid,
VF = porGrid, dx = Grid)

NH3tran <- tran.1D (C = NH3, C.up = bwNH3, D = DispNH3,
v = vGrid, VF = porGrid, dx = Grid)

CH4tran <- tran.1D (C = CH4, C.up = bwCH4, D = DispCH4, v = vGrid,
VF = porGrid, dx = Grid)

MnIItran <- tran.1D (C = MnII, C.up = bwMnII, D = DispMnII, v = vGrid,
VF = porGrid, dx = Grid)

FeIItran <- tran.1D (C = FeII, C.up = bwFeII, D = DispFeII, v = vGrid,
VF = porGrid, dx = Grid)

SO4tran <- tran.1D (C = SO4, C.up = bwSO4, D = DispSO4, v = vGrid,
VF = porGrid, dx = Grid)

H2Stran <- tran.1D (C = H2S, C.up = bwH2S, D = DispH2S, v = vGrid,
VF = porGrid, dx = Grid)

MnIIItran <- tran.1D (C = MnIII, C.up = bwMnIII, D = DispMnIII, v = vGrid,
VF = porGrid, dx = Grid)

CO3tran <- tran.1D (C = CO3, C.up = bwCO3, D = DispCO3, v = vGrid,
VF = porGrid, dx = Grid)

PO4tran <- tran.1D (C = PO4, C.up = bwPO4, D = DispPO4, v = vGrid,
```

```
VF = porGrid, dx = Grid)
if(pHincluded == 1){
Htran <- tran.1D (C = H, C.up = bwH, D = DispH, v = vGrid,
VF = porGrid, dx = Grid)}

# Biogeochemistry

# porosity factors
p2liquid    <- (1.-porGrid$mid)/porGrid$mid        # from solid -> liquid
p2solid     <- porGrid$mid/(1.-porGrid$mid)        # from liquid -> solid

# production of DIC, DIN, DIP expressed per cm3 LIQUID/day
DICprod_Min <- (rFast*FDET         + rSlow*SDET       )
DINprod_Min <- (rFast*FDET*NCrFdet + rSlow*SDET*NCrSdet)
DIPprod_Min <- (rFast*FDET*PCrFdet + rSlow*SDET*PCrSdet)

# Redox pathways
# Limitation terms
Oxicminlim <- O2/(O2 + ksO2oxic)
Denitrilim <- (1 - O2/(O2 + kinO2denit))* NO3/(NO3 + ksNO3denit)
MnO2Redlim <- (1 - O2/(O2 + kinO2mnored ))*(1 - NO3/(NO3 + kinNO3mnored))*
MnO2/(MnO2 + ksMnO2mnored)
FeOHRedlim <- (1 - O2/(O2 + kinO2feohred ))*(1 - NO3/(NO3 + kinNO3feohred))*
(1 - MnO2/(MnO2 + kinMnO2feohred))*FeOH/(FeOH + ksFeOHfeohred)
SO4RedLim  <- (1 - O2/(O2 + kinO2so4red ))*(1 - NO3/(NO3 + kinNO3so4red))*
(1 - MnO2/(MnO2 + kinMnO2so4red))*(1 - FeOH/(FeOH + kinFeOHso4red))*
SO4/(SO4 + ksSO4so4red)
MethanoLim  <- (1 - O2/(O2 + kinO2methano ))*(1 - NO3/(NO3 + kinNO3methano))*
(1 - MnO2/(MnO2 + kinMnO2methano))*(1 - FeOH/(FeOH + kinFeOHmethano))*
(1-SO4/(SO4 + kinSO4methano))

# Reaction rate expressions for primary redox species
OxicMin    <- DICprod_Min * Oxicminlim # Oxic mineralization
Denitrific <- DICprod_Min * Denitrilim # Denitrification
MnO2Red    <- DICprod_Min * MnO2Redlim # MnO2 reduction
FeOHRed    <- DICprod_Min * FeOHRedlim # FeOH reduction
SO4Red     <- so4ch4attencoef*DICprod_Min * SO4RedLim  # SO4 reduction
Methanogen <- so4ch4attencoef*DICprod_Min * MethanoLim # Methanogenesis
```

```
# Secondary Redox Reactions
Nitri      <- rnit * NH3 * O2
MnIIOx     <- rMnIIox * MnII * O2
FeIIOx     <- rFeIIox * FeII * O2
H2SOx      <- rH2Sox * H2S * O2
CH4Ox      <- rCH4ox * CH4 * O2
FeSOx      <- rFeSox * FeS * O2
FeS2Ox     <- rFeS2ox * FeS2 * O2
FeIIMnO2x  <- rFeIIMnO2x * FeII * MnO2
MnIIIOx    <- rMnIIIox * MnIII * O2
FeIIMn3x   <- rFeIIMn3x * FeII * MnIII
H2SMnO2x   <- rH2SMnO2x * H2S * MnO2
H2SMn3x    <- rH2SMn3x * H2S * MnIII
H2SFeOHx   <- rH2SFeOHx * H2S * FeOH
MnIINO3x   <- rMnIINO3x * MnII * NO3
H2SNO3x    <- rH2SNO3x * H2S * NO3
S0x        <- rS0x * S0
CH4SO4x    <- rCH4SO4x * CH4 * SO4

######################
if(pHincluded == 1){
delta1 <- as.numeric(FeII*H2S > rep(satFeS,100))
FeIIH2Sx <- delta1*rFeIIH2Sx*((FeII*H2S/(satFeS*H))-1)
FeSdiss <- (1-delta1)*rFeSdiss*FeS*(1-(FeII*H2S/(satFeS*H)))
delta2 <- as.numeric(FeII*CO3 > rep(satFeCO3,100))
FeIICO3x <- delta2*rFeIICO3x*((FeII*CO3/satFeCO3)-1)
FeCO3diss <- (1-delta2)*rFeCO3diss*FeCO3*(1-(FeII*CO3/satFeCO3))
delta3 <- as.numeric(MnII*CO3 > rep(satMnCO3,100))
MnCO3x <- delta3*rMnCO3x*((MnII*CO3/satMnCO3)-1)
MnCO3diss <- (1-delta3)*rMnCO3diss*MnCO3*(1-(MnII*CO3/satMnCO3))
} else{
FeIIH2Sx   <- rFeIIH2Sx * FeII * H2S
FeIICO3x   <- rFeIICO3x * FeII * CO3
MnCO3x     <- rMnCO3x * MnII * CO3
FeSdiss    <- rFeSdiss * FeS
FeCO3diss  <- rFeCO3diss * FeCO3
MnCO3diss  <- rMnCO3diss * MnCO3}

FeSH2Sx    <- rFeSH2Sx * FeS * H2S
```

```
# Concentration changes

dFDET <- FDETtran$dC -(OxicMin + Denitrific + MnO2Red +
FeOHRed + SO4Red + Methanogen)
dSDET <- SDETtran$dC -(OxicMin + Denitrific + MnO2Red +
FeOHRed + SO4Red + Methanogen)

dO2   <- O2tran$dC - OxicMin - 2*Nitri - MnIIOx - 5*MnIIIOx -
FeIIOx - 2*H2SOx - 2*CH4Ox - 2*FeSOx - 7*FeS2Ox

dNO3  <- NO3tran$dC - 0.8*Denitrific + Nitri - 2*MnIINO3x - H2SNO3x

dNH3  <- NH3tran$dC + ((OxicMin + Denitrific + MnO2Red +
FeOHRed + SO4Red + Methanogen)*NCrFdet  - Nitri + H2SNO3x) /
(1.+NH3Ads)

dMnO2 <- MnO2tran$dC - 2*MnO2Red - FeIIMnO2x - H2SMnO2x +
5*MnIINO3x + 4*MnIIIOx

dMnII <- MnIItran$dC + 2*MnO2Red - 4*MnIIOx + FeIIMnO2x +
FeIIMn3x + H2SMnO2x + H2SMn3x - 5*MnIINO3x - MnCO3x + MnCO3diss

dFeOH <- FeOHtran$dC - 4*FeOHRed + 4*FeIIOx + 2*FeIIMnO2x +
FeIIMn3x - 2*H2SFeOHx

dFeII <- FeIItran$dC + 4*FeOHRed - 4*FeIIOx + FeSOx + 2*FeS2Ox -
2*FeIIMnO2x - FeIIMn3x + 2*H2SFeOHx - FeIIH2Sx - FeIICO3x +
FeSdiss + FeCO3diss

dSO4  <- SO4tran$dC - 0.5*SO4Red + H2SOx + FeSOx + 4*FeS2Ox +
H2SNO3x + S0x - CH4SO4x

dH2S  <- H2Stran$dC + 0.5*SO4Red - H2SOx - H2SMnO2x - H2SMn3x -
H2SFeOHx - H2SNO3x + 3*S0x + CH4SO4x - FeIIH2Sx - FeSH2Sx + FeSdiss

dCH4  <- CH4tran$dC + 0.5*Methanogen - CH4Ox - CH4SO4x

dFeS  <- FeStran$dC - FeSOx + FeIIH2Sx - FeSH2Sx - FeSdiss
```

```
dFeS2 <- FeS2tran$dC - 2*FeS2Ox + FeSH2Sx

dMnIII<- MnIIItran$dC + 4*MnIIOx - 4*MnIIIOx - FeIIMn3x - H2SMn3x

dS0   <- S0tran$dC + H2SMnO2x + H2SMn3x + H2SFeOHx - 4*S0x

dFeCO3<- FeCO3tran$dC + FeIICO3x - FeCO3diss

dMnCO3<- MnCO3tran$dC + MnCO3x - MnCO3diss

dCO3  <- CO3tran$dC - MnCO3x - FeIICO3x + FeCO3diss + MnCO3diss

dPO4  <- PO4tran$dC + (OxicMin + Denitrific + MnO2Red + FeOHRed + SO4Red +
Methanogen)*PCrFdet + PO4adsrate*(4*FeOHRed - 4*FeIIOx - 2*FeIIMnO2x -
FeIIMn3x + 2*H2SFeOHx)

dFeP  <- FePtran$dC - PO4adsrate*4*FeOHRed + PO4adsrate*4*FeIIOx +
PO4adsrate*2*FeIIMnO2x + PO4adsrate*FeIIMn3x - PO4adsrate*2*H2SFeOHx

if(pHincluded == 1){
dH    <- Htran$dC - 0.8*Denitrific - 4*MnO2Red - 8*FeOHRed - SO4Red +
2*Nitri - 4*MnIIOx - 6*MnIIIOx + 2*H2SOx + 4*FeS2Ox - 2*H2SMnO2x +
2*H2SMn3x - 4*H2SFeOHx + 8*MnIINO3x + 2*S0x + 2*FeSH2Sx
}

# ----------------------------------------
# output variables
# ----------------------------------------

Norgflux      <- Flux*pFast*NCrFdet + Flux*(1-pFast)*NCrSdet
Norgdeepflux  <- FDETtran$flux.down*NCrFdet + SDETtran$flux.down*NCrSdet
NH3adsorption <- (DINprod_Min  - Nitri) * (1-1/(1+NH3Ads))
TOC           <- (FDET+SDET)*1200/10^9/2.5  #  excess organic carbon

# Model output
return(list(
c(dFDET, dSDET, dO2, dNO3, dNH3, dCH4, dMnO2, dMnII, dFeOH, dFeII,
dSO4, dH2S, dFeS, dFeS2, dMnIII, dS0, dFeCO3, dMnCO3, dCO3, dPO4,
```

```
dFeP, if(pHincluded == 1){dH}),    # derivatives
TOC  = TOC,                        # excess organic carbon

# Fluxes
Norgflux = Norgflux,
Norgdeepflux = Norgdeepflux,
O2flux = O2tran$flux.up,
O2deepflux = O2tran$flux.down,
NO3flux = NO3tran$flux.up,
NO3deepflux = NO3tran$flux.down,
NH3flux = NH3tran$flux.up*(1+NH3Ads),
NH3deepflux = NH3tran$flux.down*(1+NH3Ads),
CH4flux = CH4tran$flux.up,
CH4deepflux = CH4tran$flux.down,
MnO2flux = MnO2tran$flux.up,
MnO2deepflux = MnO2tran$flux.down,
MnIIflux = MnIItran$flux.up,
MnIIdeepflux = MnIItran$flux.down,
FeOHflux = FeOHtran$flux.up,
FeOHdeepflux = FeOHtran$flux.down,
FeIIflux = FeIItran$flux.up,
FeIIdeepflux = FeIItran$flux.down,
SO4flux = SO4tran$flux.up,
SO4deepflux = SO4tran$flux.down,
H2Sflux = H2Stran$flux.up,
H2Sdeepflux = H2Stran$flux.down,
FeSflux = FeStran$flux.up,
FeSdeepflux = FeStran$flux.down,
FeS2flux = FeS2tran$flux.up,
FeS2deepflux = FeS2tran$flux.down,
MnIIIflux = MnIIItran$flux.up,
MnIIIdeepflux = MnIIItran$flux.down,
S0flux = S0tran$flux.up,
S0deepflux = S0tran$flux.down,
FeCO3flux = FeCO3tran$flux.up,
FeCO3deepflux = FeCO3tran$flux.down,
MnCO3flux = MnCO3tran$flux.up,
MnCO3deepflux = MnCO3tran$flux.down,
CO3flux = CO3tran$flux.up,
```

```
CO3deepflux = CO3tran$flux.down,
PO4flux = PO4tran$flux.up,
PO4deepflux = PO4tran$flux.down,
FePflux = FePtran$flux.up,
FePdeepflux = FePtran$flux.down,
if(pHincluded == 1){Hflux = Htran$flux.up},
if(pHincluded == 1){Hdeepflux = Htran$flux.down},

# rate profiles
NH3adsorption = NH3adsorption, OxicMin = OxicMin, Denitrific = Denitrific,
Methanogen = Methanogen, MnO2Red = MnO2Red,FeOHRed = FeOHRed,
SO4Red = SO4Red, Nitri = Nitri,MnIIOx = MnIIOx,
FeIIOx = FeIIOx, H2SOx = H2SOx,CH4Ox = CH4Ox,
FeSOx = FeSOx, FeS2Ox = FeS2Ox,MnIIIOx = MnIIIOx,
FeIIMn3x = FeIIMn3x, H2SMnO2x = H2SMnO2x, H2SMn3x = H2SMn3x,
H2SFeOHx = H2SFeOHx, MnIINO3x = MnIINO3x, H2SNO3x = H2SNO3x,
S0x = S0x, CH4SO4x = CH4SO4x, FeIIH2Sx = FeIIH2Sx,
FeSH2Sx = FeSH2Sx, FeIICO3x = FeIICO3x,MnCO3x = MnCO3x,
FeSdiss = FeSdiss, FeCO3diss = FeCO3diss, MnCO3diss = MnCO3diss,
FeIIMnO2x = FeIIMnO2x, FeIItran = FeIItran,FeOHtran = FeOHtran,
NO3tran = NO3tran, MethanoLim = MethanoLim, DICprod_Min = DICprod_Min,
dFeOH = dFeOH))
})

}
require(ReacTran) # Reactive transport package
require(marelac) # Diffusion coefficient package

# Physical Conditions
Temp <- 5
Sal  <- 35
por  <- 0.4
Press <- 10.1325

# Transport Properties

# Grid: 100 layers; total length=50 cm, first box=0.01 cm
Grid  <- setup.grid.1D(N = 100, dx.1 = 0.01, L = 50)
Depth <- Grid$x.mid
```

```
N     <- Grid$N

# porosity: fixed and constant value
# porGrid <- setup.prop.1D(value = por, grid = Grid)

# porosity as function of depth
porinf <- 0.79    # porosity at infinite depth
porzero <- 0.9    # porosity at the sediment-water interface
beta <- 0.25      # porosity depth attenuation coefficient

porfunc <- function(x, y0, yinf, xatt)
return(yinf + (y0-yinf)*exp(-xatt*x))

porGrid <- setup.prop.1D(func = porfunc, y0 = porzero,
yinf = porinf, xatt = beta, grid = Grid)
porGridSolid <- setup.prop.1D(value= 0, grid = Grid )
porGridSolid$int <- 1- porGrid$int
porGridSolid$mid <- 1- porGrid$mid

# Diffusion coefficients are calculated using 'marelac' package
DiffCoeffs <- diffcoeff(S = Sal, t = Temp,
 P = Press)*3600*24*1e4 # from m2/s -> cm2/d

# Include Tortuosity:
diffmat <- list()
for( i in colnames(DiffCoeffs)){
tortfunc <- function(x, y0, yinf, xatt, coefff){
return(as.numeric(coefff)/(1-log((yinf + (y0-yinf)*exp(-xatt*x))^2)))
}
diffmat[[i]] <- setup.prop.1D(func = tortfunc, y0 = porzero,
yinf = porinf, xatt = beta, coeff = DiffCoeffs[i], grid = Grid)
}
# for multiplying porosity and diffusion coefficient
# and adding up bioturbation to diffusion in prop class
difporbiotf <- function(i){
trnsprt <- setup.prop.1D(value = 0, grid = Grid)
trnsprt$int <- diffmat[[i]]$int * porGrid$int + DbGrid$int
trnsprt$mid <- diffmat[[i]]$mid * porGrid$mid + DbGrid$mid
return(trnsprt)}
```

```
#Diffusion Coefficients:
DispO2      <- difporbiotf('O2')
DispNO3     <- difporbiotf('NO3')
DispNH3     <- difporbiotf('NH3')
DispNH3$mid <- DispNH3$mid/(1+NH3Ads)
DispNH3$int <- DispNH3$int/(1+NH3Ads)
DispCH4     <- difporbiotf('CH4')
DispMnII    <- difporbiotf('Mn')
DispFeII    <- difporbiotf('Fe')
DispSO4     <- difporbiotf('SO4')
DispH2S     <- difporbiotf('H2S')
DispMnIII   <- difporbiotf('Mn')
DispCO3     <- difporbiotf('CO3')
DispPO4     <- difporbiotf('PO4')
DispH       <- difporbiotf('H')

# Bioturbation:
biot <- 5/365           # cm2/d      - bioturbation coefficient
mixL <- 10              # cm         - depth of mixed layer

exp.profile <- function(x, y.0, x.att)
return(y.0*exp(x^2/(2*x.att^2)))
DbGrid <- setup.prop.1D(func = exp.profile,
y.0 = biot, x.att = mixL,
grid = Grid)
DbGrid$int <- DbGrid$int* porGrid$int
DbGrid$mid <- DbGrid$mid* porGrid$mid

# Burial Velocities:
uinf <- 0.2       # burial velocity of solids at infinite depth
ufunc <- function(x, yinf, porinf)
return(yinf*porinf)
uGrid <- setup.prop.1D(func = ufunc, yinf = uinf,
porinf = 1 - porinf, grid = Grid)  # solid burial velocity
uGrid$mid <- uGrid$mid/(porGridSolid$mid*365)
uGrid$int <- uGrid$int/(porGridSolid$int*365)

vGrid <- setup.prop.1D(func = ufunc, yinf = uinf,
```

```
porinf = porinf, grid = Grid)  # solute burial velocity
vGrid$mid <- vGrid$mid/(porGrid$mid*365)
vGrid$int <- vGrid$int/(porGrid$int*365)

# organic matter dynamics  #
MeanFlux <- 15000/12*100/365  # nmol/cm2/d - C deposition: 5gC/m2/yr
rFast    <- 1.3/365              #/day        - decay rate fast decay det.
rSlow    <- 0.01/365             #/day        - decay rate slow decay det.
pFast    <- 0.5              #-           - fraction fast det. in flux
w        <- 0.5/365          # cm/d       - advection rate
NCrFdet  <- 0.169            # molN/molC  - NC ratio fast decay det.
NCrSdet  <- 0.169            # molN/molC  - NC ratio slow decay det.
PCrFdet  <- 0.009            # molP/molC  - PC ratio fast decay
PCrSdet  <- 0.009            # molP/molC  - PC ratio slow decay

# Nutrient bottom water conditions (mmol/m3)
bwO2       <- 6
bwNO3      <- 25
bwNH3      <- 0.
bwCH4      <- 0.
bwMnO2     <- 10
bwMnII     <- 0.
bwFeOH     <- 0.1
bwFeII       <- 0.
bwSO4      <- 28.7
bwH2S      <- 0
bwFeS      <- 0
bwFeS2     <- 0
bwMnIII    <- 0.
bwS0       <- 0
bwFeCO3    <- 0
bwMnCO3    <- 0
bwCO3      <- 1
bwPO4      <- 0.002
bwFeP      <- 0
bwH <- 1000
# Nutrient parameters
NH3Ads     <- 1.3    #-           Adsorption coeff ammonium
rnit       <- 100000/365     #/d          Max nitrification rate
```

```
rCH4ox     <- 100000/365.     #/d          Max rate oxidation of CH4
ksO2oxic   <- 1.      #mmolO2/m3   half-sat O2 in oxic mineralis
ksNO3denit <- 4.      #mmolNO3/m3  half-sat NO3 in denitrif
kinO2denit <- 10.      #mmolO2/m3   half-sat O2 inhib denitrif
kinNO3methano <- 5.      #mmolNO3/m3  half-sat NO3 inhib anoxic min
kinO2methano  <- 5.      #mmolO2/m3   half-sat O2 inhib anoxic min

rMnIIox      <- 100000/365
ksMnO2mnored <- 4.
kinO2mnored  <- 10.
kinNO3mnored <- 5.
kinMnO2methano <- 1.
rFeIIox      <- 35000/365
ksFeOHfeohred <- 60.
kinO2feohred  <- 10.
kinNO3feohred <- 5.
kinMnO2feohred <- 1.
kinFeOHmethano <- 1.
rH2Sox       <- 16000/365
ksSO4so4red <- 1.
kinO2so4red  <- 10.
kinNO3so4red <- 5.
kinMnO2so4red <- 1.
kinFeOHso4red <- 1.
kinSO4methano <- 1.
rFeSox <- 1000/365
rFeS2ox <- 20/365
rFeIIMnO2x <- 10/365
rMnIIIox      <- 100000/365
rFeIIMn3x <- 0.03
rH2SMnO2x <- 20/365
rH2SMn3x <- 0.01
rH2SFeOHx <-10/365
rMnIINO3x <- 10000/365
rH2SNO3x <- 10000/365
rS0x <- 0.1/365
rCH4SO4x <- 10/365
rFeIIH2Sx <- 1000/365
kFeS <- 0.1
```

```
rFeSH2Sx <- 200/365
rFeIICO3x <- 10/365
rMnCO3x <- 1/365
rFeSdiss <- 100/365
rFeCO3diss <- 100/365
rMnCO3diss <- 0.25/365
satFeS <- 1e-04
satFeCO3 <- 1e-04
satMnCO3 <- 1e-04
PO4adsrate <- 0.01
so4ch4attencoef <- 0.075

#### input parameters to be adjusted in the implementation part
pars <- c(
MeanFlux   =  MeanFlux   ,rFast     =  rFast      ,
rSlow      =  rSlow      ,pFast     =  pFast      ,
w          =  w          ,NCrFdet   =  NCrFdet    ,
NCrSdet    =  NCrSdet    ,bwO2      =  bwO2       ,
bwNO3      =  bwNO3      ,bwNH3     =  bwNH3      ,
bwCH4      =  bwCH4      ,NH3Ads    =  NH3Ads      ,
rnit       =  rnit       ,#ksO2nitri =  ksO2nitri  ,
rCH4ox     =  rCH4ox     ,#ksO2ch4ox =  ksO2ch4ox  ,
ksO2oxic   =  ksO2oxic   ,ksNO3denit=  ksNO3denit ,
kinO2denit =  kinO2denit ,kinNO3methano=  kinNO3methano ,
kinO2methano  =  kinO2methano, rMnIIox = rMnIIox,
ksMnO2mnored = ksMnO2mnored, kinO2mnored = kinO2mnored,
kinNO3mnored = kinNO3mnored, kinMnO2methano = kinMnO2methano,
bwMnO2 = bwMnO2, bwMnII=bwMnII, rFeIIox = rFeIIox,
ksFeOHfeohred = ksFeOHfeohred, kinO2feohred = kinO2feohred,
kinNO3feohred = kinNO3feohred, kinMnO2feohred = kinMnO2feohred,
kinFeOHmethano = kinFeOHmethano, bwFeOH = bwFeOH,
bwFeII=bwFeII, rH2Sox = rH2Sox, ksSO4so4red = ksSO4so4red,
kinO2so4red = kinO2so4red, kinNO3so4red = kinNO3so4red,
kinMnO2so4red = kinMnO2so4red, kinFeOHso4red = kinFeOHso4red,
kinSO4methano = kinSO4methano, bwSO4 = bwSO4, bwH2S = bwH2S,
rFeSox = rFeSox, bwFeS = bwFeS, rFeS2ox = rFeS2ox,
bwFeS2 = bwFeS2, rMnIIIox = rMnIIIox, bwMnIII = bwMnIII,
rFeIIMn3x = rFeIIMn3x, rFeIIMnO2x = rFeIIMnO2x,
rH2SMnO2x = rH2SMnO2x, rH2SMn3x = rH2SMn3x,
```

```
rH2SFeOHx = rH2SFeOHx, rMnIINO3x = rMnIINO3x,
rH2SNO3x = rH2SNO3x, rS0x = rS0x, bwS0 = bwS0,
rCH4SO4x = rCH4SO4x, rFeIIH2Sx = rFeIIH2Sx,
rFeSH2Sx= rFeSH2Sx, rFeIICO3x = rFeIICO3x,
bwFeCO3 = bwFeCO3, bwCO3 = bwCO3,
rMnCO3x = rMnCO3x, bwMnCO3 = bwMnCO3,
bwH = bwH, bwPO4 = bwPO4, bwFeP = bwFeP,
biot = biot, mixL = mixL, Temp = Temp, satFeS = satFeS,
so4ch4attencoef = so4ch4attencoef, satFeCO3 = satFeCO3,
rFeCO3diss = rFeCO3diss, rMnCO3diss = rMnCO3diss,
satMnCO3 = satMnCO3, rFeSdiss = rFeSdiss, PO4adsrate = PO4adsrate)

# names of state variables and initial conditions
svarnames <- c("FDET", "SDET", "O2", "NO3", "NH3", "CH4", "MnO2",
"MnII", "FeOH", "FeII", "SO4", "H2S", "FeS", "FeS2",
"MnIII", "S0", "FeCO3", "MnCO3", "CO3", "PO4", "FeP",
if(pHincluded==1){"H"})
nspec     <- length(svarnames)
Cini      <- rep(10, N*nspec)

################## RUNNING THE MODEL ############################

print(Sys.time())

pars1 <- pars
#@@@@@@@@@@ Madison Data @@@@@@@@@@@@@@@@
pars1["biot"] <- 5/365
pars1["pFast"] <- 1/8
pars1["MeanFlux"] <- 29000/12*100/365
pars1["bwO2"] <- 295
pars1["bwNO3"] <- 25
pars1["bwFeOH"] <- 50#5/365
pars1["bwMnO2"] <- 8#0.9/365
pars1["bwPO4"] <- 4.
pars1["bwNH3"] <- 0.
pars1["bwH2S"] <- 0.
pars1["bwMnII"] <- 0.
pars1["bwMnIII"] <- 0.
pars1["bwFeII"] <- 0.
```

```
pars1["bwCH4"] <- 0.
pars1["bwFeS"] <- 0.
pars1["bwS0"] <- 0.
pars1["bwFeS2"] <- 0.
pars1["bwMnCO3"] <- 0.
pars1["bwFeCO3"] <- 0.
pars1["bwSO4"] <- 28700
pars1["ksO2oxic"] <- 1
pars1["ksNO3denit"] <- 4
pars1["ksMnO2mnored"] <- 4
pars1["ksFeOHfeohred"] <- 60
pars1["ksSO4red"] <- 1000
pars1["rFast"] <- 1.3/365
pars1["rSlow"] <- 0.01/365
pars1["rnit"] <- 100/365
pars1["rMnIIOx"] <- 1000/365
pars1["rMnIIIOx"] <- 100/365
pars1["rFeIIOx"] <- 35/365
pars1["rH2SOx"] <- 16/365
pars1["rCH4Ox"] <- 100/365
pars1["rFeSOx"] <- 1/365
pars1["rFeS2Ox"] <- 0.02/365
pars1["rFeIIMnO2x"] <- 0.01/365
pars1["rFeIIMn3x"] <- 1/365
pars1["rH2SMnO2x"] <- 0.02/365
pars1["rH2SMn3x"] <- 0
pars1["rMnIINO3x"] <- 10/365
pars1["rH2SNO3x"] <- 10/365
pars1["rS0x"] <- 0.1/365
pars1["rH2SFeOHx"] <- 0.01/365
pars1["rFeSH2Sx"] <- 0.000001/365#0.2/365
pars1["rCH4SO4x"] <- 0.000001/365#0.01/365
pars1["rFeIIH2Sx"] <- 0.01/365 #1/365
pars1["rMnCO3x"] <- 0.01/365
pars1["satMnCO3"] <- 3*10^-9
pars1["rMnCO3diss"] <- 0.25/365
pars1["rFeIICO3x"] <- 0.01/365
pars1["satFeCO3"] <- 4*10^-9
pars1["rFeCO3diss"] <- 0.25/365
```

```
pars1["NH3Ads"] <- 1.4
pars1["so4ch4attencoef"] <- 0.0 # S3 0 # S2 0.000075 # S1 0.075
pars1["PO4adsrate"] <- 0.01
pars1["bwFeP"] <- pars1["bwFeOH"]*pars1["PO4adsrate"]
# Wijsman
pars1["kinO2denit"] <- 1
pars1["kinO2mnored"] <- 8
pars1["kinO2feohred"] <- 8
pars1["kinO2so4red"] <- 8
pars1["kinNO3mnored"] <- 0.01
pars1["kinNO3feohred"] <- 0.01
pars1["kinNO3so4red"] <- 10
pars1["kinNO3methano"] <- 0.01
pars1["kinMnO2feohred"] <- 5
pars1["kinMnO2so4red"] <- 5000
pars1["kinMnO2methano"] <- 5000
pars1["kinFeOHso4red"] <- 12500
pars1["kinFeOHmethano"] <- 12500
pars1["kinSO4methano"] <- 1000

print(system.time(
DIA1  <- steady.1D (y = Cini, func = OMEXDIA_kb, names = svarnames,
parms = pars1, nspec = nspec, positive = TRUE,
method = 'runsteady')
))

pars2 <- pars
pars2 = pars1
pars2["bwO2"] <- 140

print(system.time(
DIA2  <- steady.1D (y = Cini, func = OMEXDIA_kb, names = svarnames,
parms = pars2, nspec = nspec, positive = TRUE,
method = 'runsteady')
))

pars3 <- pars
pars3 = pars1
pars3["bwO2"] <- 80
```

```
print(system.time(
DIA3  <- steady.1D (y = Cini, func = OMEXDIA_kb, names = svarnames,
parms = pars3, nspec = nspec, positive = TRUE,
method = 'runsteady')
))

pars4 <- pars
pars4 = pars1
pars4["bwO2"] <- 40

print(system.time(
DIA4  <- steady.1D (y = Cini, func = OMEXDIA_kb, names = svarnames,
parms = pars4, nspec = nspec, positive = TRUE,
method = 'runsteady')
))

pars5 <- pars
pars5 = pars1
pars5["bwO2"] <- 5

print(system.time(
DIA5  <- steady.1D (y = Cini, func = OMEXDIA_kb, names = svarnames,
parms = pars5, nspec = nspec, positive = TRUE)#, method = 'runsteady',
method = 'runsteady')
))

#====================#
# Plotting           #
#====================#

par(mfrow=c(5,4))
plot(DIA1,DIA2,DIA3,DIA4,DIA5,
which = c("O2", "NO3", "NH3", "MnO2", "MnII", "FeOH",
"FeII","SO4","H2S","CH4","FeS","FeS2",
"MnIII", "S0", "PO4", "MnCO3", "FeCO3", "TOC","FeP"),
ylim = list(c(2, 0), c(2, 0), c(50,0), c(2,0),
c(50,0),c(2,0), c(50,0), c(50,0),c(50,0), c(50,0),
c(50,0), c(50,0), c(10,0), c(50,0), c(10,0),c(50,0),
```

```
c(50,0), c(10,0),c(2,0)),
grid = Grid$x.mid, lwd = 2, xlab = c(rep("mmol/m3",17),
"%","mmol/m3"),
xyswap = TRUE, ylab = "depth, cm",
obspar = list(pch = ".", cex = 3), mfrow = NULL)
plot.new()
o2conc <- c(pars1["bwO2"], pars2["bwO2"], pars3["bwO2"], pars4["bwO2"],
pars5["bwO2"])
# legtext <- paste(formatC(CFlux, 3), "gC/m2/yr")
legtext <- paste(formatC(o2conc, 3), "")
legend ("bottom", col = 1:5, lty = 1:5, lwd = 4, cex= 1,
legend = legtext, ncol = 2)#, title = "O2 conc(uM)")

# mtext(outer = TRUE, side = 3, line = -1.5, cex = 1, "Model Output")

########### mineralization rates ###############

minrates <- matrix(data = c(sum(DIA1$OxicMin), sum(DIA1$Denitrific),
sum(DIA1$MnO2Red),sum(DIA1$FeOHRed), sum(DIA1$SO4Red),
sum(DIA1$Methanogen), sum(DIA2$OxicMin), sum(DIA2$Denitrific),
sum(DIA2$MnO2Red), sum(DIA2$FeOHRed), sum(DIA2$SO4Red),
sum(DIA2$Methanogen), sum(DIA3$OxicMin), sum(DIA3$Denitrific),
sum(DIA3$MnO2Red), sum(DIA3$FeOHRed), sum(DIA3$SO4Red),
sum(DIA3$Methanogen), sum(DIA4$OxicMin), sum(DIA4$Denitrific),
sum(DIA4$MnO2Red), sum(DIA4$FeOHRed), sum(DIA4$SO4Red),
sum(DIA4$Methanogen), sum(DIA5$OxicMin), sum(DIA5$Denitrific),
sum(DIA5$MnO2Red), sum(DIA5$FeOHRed), sum(DIA5$SO4Red),
sum(DIA5$Methanogen)), nrow = 5,byrow = 1)
colnames(minrates) <- c("Oxic Min.", "Denit.", "MnO2 Red.",
"FeOH Red.", "SO4 Red.", "Methanogen.")
rownames(minrates) <- c(paste("BW O2 (uM) =", pars1["bwO2"]),
paste("BW O2 (uM) =", pars2["bwO2"]), paste("BW O2 (uM) =",
pars3["bwO2"]), paste("BW O2 (uM) =", pars4["bwO2"]),
paste("BW O2 (uM) =", pars5["bwO2"]))
minratesperc <- minrates
minratesperc <- round(minrates/rowSums(minrates), 4)
minratesperc

# ############# flux rates ###################
```

```
fluxes <- matrix(data = c(DIA1$PO4flux, DIA2$PO4flux,DIA3$PO4flux,
DIA4$PO4flux, DIA5$PO4flux,DIA1$NH3flux, DIA2$NH3flux,DIA3$NH3flux,
DIA4$NH3flux, DIA5$NH3flux, DIA1$NO3flux, DIA2$NO3flux,DIA3$NO3flux,
DIA4$NO3flux, DIA5$NO3flux, DIA1$H2Sflux, DIA2$H2Sflux,DIA3$H2Sflux,
DIA4$H2Sflux, DIA5$H2Sflux, DIA1$MnIIflux, DIA2$MnIIflux,DIA3$MnIIflux,
DIA4$MnIIflux, DIA5$MnIIflux, DIA1$MnIIIflux, DIA2$MnIIIflux,DIA3$MnIIIflux,
DIA4$MnIIIflux, DIA5$MnIIIflux, DIA1$FeIIflux, DIA2$FeIIflux,DIA3$FeIIflux,
DIA4$FeIIflux, DIA4$FeIIflux), nrow = 5)
rownames(fluxes) <- rownames(minrates)
colnames(fluxes) <- c("PO4 flux", "NH3 flux", "NO3 flux",
"H2S flux", "MnII flux", "MnIII flux", "FeII flux")
fluxes
npratio <- (fluxes[,"NH3 flux"] + fluxes[,"NO3 flux"])/fluxes[,"PO4 flux"]
```